

⁵ Department of Earth and Ocean Sciences, 6339 Stores Road, University of British Columbia, Vancouver, BC, V6T 1Z4, Canada

⁶ Department of Zoology, University of Fort Hare, Private Bag X1314, Alice 5700, South Africa

Received: 18 June 2010 – Accepted: 30 June 2010 – Published: 23 July 2010

Correspondence to: S. J. Thomalla (sandy.thomalla@gmail.com)

Published by Copernicus Publications on behalf of the European Geosciences Union.

OSD

7, 1347–1403, 2010

Phytoplankton distribution and nitrogen dynamics in the Southern Ocean

S. J. Thomalla et al.

Title Page

Abstract

Introduction

Conclusions

References

Tables

Figures

⏪

⏩

◀

▶

Back

Close

Full Screen / Esc

Printer-friendly Version

Interactive Discussion



Abstract

During the 1999 Marion Island Oceanographic Survey (MIOS 4) in late austral summer, a northbound and reciprocal southbound transect were taken along the Southwest Indian and Madagascar Ridge, between the Prince Edward Islands and 31° S. The sections crossed a number of major fronts and smaller mesoscale features and covered a wide productivity spectrum from subtropical to subantarctic waters. Associated with the physical survey were measurements of size fractionated chlorophyll, nutrients and nitrogen (NO_3 , NH_4 and urea) uptake rates. Subtropical waters were characterised by low concentrations ($<0.27 \text{ mg m}^{-3}$) of pico-phytoplankton cells ($>81\%$) and very low f -ratios (<0.1), indicative of productivity based almost entirely on recycled ammonium and urea. Diatom growth was limited by the availability of NO_3 ($<1 \text{ mmol m}^{-3}$) and SiO_4 ($<1.5 \text{ mmol m}^{-3}$) through vertical stratification that prevents the upward flux of nutrients into the euphotic zone. Biomass accumulation of small cells was likely controlled by microzooplankton grazing. In subantarctic waters, total chlorophyll concentrations increased ($<0.74 \text{ mg m}^{-3}$) and larger cells became more prevalent, however smaller phytoplankton cells and low f -ratios (>0.15) still dominated, despite sufficient NO_3 availability. The results from this study favour Si limitation, light-limited deep mixing and likely Fe deficiency as the dominant mechanisms controlling significant new production by micro-phytoplankton. Increased concentrations of micro-phytoplankton cells and rates of new production did however occur at oceanic frontal regions (58.6% and 11.22%, respectively), and in the region of the Prince Edward archipelago (61.4% and 14.16%, respectively). Here water column stabilization and local Fe-enrichment are thought to stimulate phytoplankton growth rates, especially of diatoms. Open ocean regions such as these provide important areas for local but significant POC export and biological CO_2 draw-down in an overall HNLC Southern Ocean.

Phytoplankton distribution and nitrogen dynamics in the Southern Ocean

S. J. Thomalla et al.

Title Page

Abstract

Introduction

Conclusions

References

Tables

Figures



Back

Close

Full Screen / Esc

Printer-friendly Version

Interactive Discussion



1 Introduction

The “biological carbon pump” (Volk and Hoffert, 1985; Longhurst, 1991; Falkowski and Raven, 1997) provides the link between the atmospheric and oceanic carbon cycles, primarily through phytoplankton photosynthesis and carbon export processes. The biological pump plays an important role in ameliorating current increases in atmospheric CO₂ by removing an estimated 10 GtC (1 GtC=10¹⁵ g of carbon) from surface waters of the world’s oceans each year (Falkowski et al., 1998). The rate at which inorganic carbon is fixed into particulate and dissolved organic carbon (POC, DOC) that sinks, or is otherwise transported through the water column to below the seasonal thermocline, sets the strength of the biological carbon pump. Thus factors that regulate phytoplankton growth (light, nutrients), particle formation and rates of sinking (aggregation, ballasting, senescence, grazing) and remineralisation (bacterial activity, chemical dissolution) all modify POC and DOC fluxes and therefore the strength of the biological carbon pump.

The Sub-Antarctic region of the Southern Ocean is one of the largest oceanic sinks for atmospheric CO₂ (Metzl et al., 1999), while the SW Indian Ocean region is infrequently sampled (Lucas et al., 2007) and for both regions, direct measurements of carbon export are relatively few. Measurements of export production have been made directly by sediment trap (e.g., Honjo et al., 2000; Salter et al., 2007) and indirectly by thorium isotopes (e.g., Cochran et al., 2000; Morris et al., 2007), by calculating NO₃ “draw down” (Koeve, 2001; Rubin, 2003; Sanders et al., 2005, 2007) and by using ¹⁵N stable isotopes that differentiate between “new” (export) and “regenerated” (recycled) production (Dugdale and Goering, 1967; Eppley and Peterson, 1979; Bury et al., 1995; Waldron et al., 1995). Partitioning between new and regenerated nitrogen uptake is quantified by the *f*-ratio, a measure of that fraction of “new” primary production that is available for export to the deep ocean or to higher trophic levels, relative to “regenerated” production which supports planktonic community maintenance requirements (Tremblay et al., 1997). *f*-ratio calculations rely on assumptions of steady state, no

Phytoplankton distribution and nitrogen dynamics in the Southern Ocean

S. J. Thomalla et al.

Title Page

Abstract

Introduction

Conclusions

References

Tables

Figures



Back

Close

Full Screen / Esc

Printer-friendly Version

Interactive Discussion



storage of N in surface waters (Eppley and Peterson, 1979; Eppley, 1989; Knauer et al., 1990) and minimal euphotic layer nitrification (Fernandez and Raimbault, 2007; Yool et al., 2007). In the open oceans, nitrification was originally thought to be confined to the deeper, aphotic layers of the water column due to light inhibition (Olson, 1981). However, recent findings of significant rates of euphotic nitrification, particularly in oligotrophic rather than nutrient rich polar oceans, can severely hinder the use of the f -ratio for diagnosing export production (Dore and Karl, 1996; Raimbault et al., 1999; Diaz and Raimbault, 2000; Rees et al., 2002; Fernandez and Raimbault, 2007; Yool et al., 2007). Further problems arise when expressing PON export in carbon terms as phytoplankton growth frequently follows non-Redfield ratios because of disturbances to cellular Redfield elemental stoichiometry by light and/or available Si and Fe (Geider and La Roche, 2002; Timmermans et al., 2004; Hoffmann et al., 2006; Moore et al., 2007b). Thus use of the f -ratio to estimate export production from the euphotic layer must now be considered with circumspection although in HNLC environments, the f -ratio can be an instructive diagnostic tool for evaluating the potential for Fe-limited nitrate uptake (Lucas et al., 2007).

Iron limited phytoplankton production in HNLC environments is now unequivocally established through a number of artificial iron fertilisation experiments (De Baar et al., 2005; Boyd et al., 2007) while two natural iron fertilization experiments in the Southern Ocean (KEOPS: Blain et al., 2001 and CROZEX: Pollard et al., 2007) have further assessed the impact of Fe-fertilisation on carbon export and the carbon to iron (C:Fe) export efficiency. Regions of relative iron availability are characterized by larger average cell sizes, a dominance by diatoms, higher f -ratios, faster rates of specific nitrate uptake ($V_{NO_3} d^{-1}$), lower POC:chl- a ratios and improved photo-physiological competency as revealed by FRRf values for Fv/Fm. All these parameters provide physiological and taxonomic evidence for the impact of Fe availability, which increases with proximity to Sub-Antarctic Islands such as the Crozet and Kerguelen archipelagos (Blain et al., 2001; Lucas et al., 2007; Moore et al., 2007a,b; Pollard et al., 2007; Poulton et al., 2007; Seeyave et al., 2007). Indeed, ocean colour satellite imagery demonstrates

Phytoplankton distribution and nitrogen dynamics in the Southern Ocean

S. J. Thomalla et al.

[Title Page](#)[Abstract](#)[Introduction](#)[Conclusions](#)[References](#)[Tables](#)[Figures](#)[⏪](#)[⏩](#)[◀](#)[▶](#)[Back](#)[Close](#)[Full Screen / Esc](#)[Printer-friendly Version](#)[Interactive Discussion](#)

the 1999 cruise (MIOS 4), an additional northbound (Fig. 1a) and a reciprocal southbound transect (Fig. 1b) followed the Southwest Indian and Madagascar Ridge, between the Prince Edward Islands and 31° S. This section crossed a number of major fronts and smaller, mesoscale features. Associated with this physical survey, measurements of chlorophyll (chl-*a*), nutrient concentrations and phytoplankton nitrogen uptake were also performed.

Northbound transect

During the northbound transect, the water column temperature structure was determined from 68 Sippican T-7 (to 760 m) XBT deployments at 15' latitude intervals (Fig. 1a). Temperature profiles were plotted as sections in Ocean Data View (ODV) (Schlitzer, 2004) to locate the frontal positions and hence plan the CTD station spacing for the southbound leg. To identify the major features along the Madagascar Ridge section, the definitions of the frontal positions outlined by Park et al. (1993) were adopted. They defined these features using the subsurface (200 m) cross frontal ranges of temperature as well as their axial values. The AF was identified by a temperature range of 12–16°C (median 14°C), the STF by 8–12°C (median 10°C) and the SAF by 4–8°C (median 6°C). On this northbound transect, surface samples were taken for total and size fractionated chl-*a* determinations.

Southbound transect

The southbound section consisted of 33 CTD profiles (to ~2000 m) that was worked close to the crest of the ridge running south from Madagascar to the crest of the Southwest Indian Ridge before turning south-west and terminating west of the Prince Edward Islands (Fig. 1b). Station spacing varied from 1° over the subtropical gyre between 31° and 37° S to every 20' latitude over the frontal regions. Water samples were collected from 12 standard depths between 2000 m and the surface. Productivity stations were carried out at selected locations (Table 1) where a second CTD cast was deployed. At each station, light attenuation was estimated by Secchi disk because of a malfunctioning underwater PAR sensor. The extinction coefficient K_d was used to calculate the

Phytoplankton distribution and nitrogen dynamics in the Southern Ocean

S. J. Thomalla et al.

Title Page

Abstract

Introduction

Conclusions

References

Tables

Figures



Back

Close

Full Screen / Esc

Printer-friendly Version

Interactive Discussion



100, 50, 25, 10, 1 and 0.1% light depths from:

$$Z(x\%) = \frac{Z(sd)}{1.44(-\ln(x/100))}$$

Where: $Z(x\%)$ is the depth (m) of a particular light level ($x\%$), $Z(sd)$ is the Secchi depth (m) and x is the light level to be determined.

2.1 Chlorophyll-*a*

Samples from the 6 light depths to 150 m were pre-screened through a 200 μm mesh to exclude zooplankton grazers, after which they were gently filtered (<5 cm Hg) through a serial filtration unit and fractionated into pico- (<2.0 μm), nano- (2–20 μm) and micro-phytoplankton (>20–200 μm) size fractions and collected on 25 mm Whatman GF/F filters. After extraction in 90% acetone for 24 h, chlorophyll-*a* was measured on an AU-10 Turner Designs fluorometer, calibrated against a standard chlorophyll-*a* solution (Sigma).

2.2 Nutrients

A 15 ml sample from every depth was stored frozen for later nutrient analysis back at the University of Cape Town (UCT). Manual analyses were performed for NO_3 and Si according to the methods described in Grasshoff et al. (1983) and Parsons et al. (1984), but scaled to a 5 ml sample size. For each productivity station, on board analyses of ammonium and urea were carried out in triplicate for each light depth according to the manual method described in Grasshoff et al. (1983), but scaled down to 5 ml sample volumes.

2.3 ^{15}N incubations

Bulk water samples were obtained from each of the six light depths and dispensed into three 2 l acid cleaned glass Schotte bottles for NO_3^- , NH_4^+ and urea uptake

measurements. Spikes at ~10% of ambient concentration for $^{15}\text{N-NO}_3$, $^{15}\text{N-NH}_4$ and $^{15}\text{N-urea}$ were added to one of each of the three 2l incubation bottles. These were transferred into on-deck perspex tube incubators, screened with neutral density filters to simulate in situ light at the appropriate depths. Ambient in situ temperatures were maintained by pumping surface seawater through the incubators. The samples were incubated for between 10–24 h, centred around local midday. Isotopic-dilution of $^{15}\text{N-NH}_4$ in particular by NH_4 excretion in vitro will underestimate the computed NH_4 uptake rates (Harrison and Harris, 1986; Donald et al., 2001; Varela et al., 2005), particularly in oligotrophic oceans (Harrison and Harris, 1986). Uptake experiments were terminated by filtration onto ashed 47 mm GF/F filters that were then stored at -20°C for later analysis at the Plymouth Marine Laboratory (PML) for particulate nitrogen and atom% ^{15}N analyses on a Europa Tracermass continuous flow mass spectrometer (Europa Scientific Ltd.) using methods described by Barrie et al. (1989) and Owens and Rees (1989).

Nitrate, urea and ammonium uptake rates were calculated according to Dugdale and Goering (1967):

$$\rho\text{NO}_3, \rho\text{NH}_4 \text{ and } \rho\text{urea} (\text{mmol m}^{-3} \text{ h}^{-1}) = (\text{PE} \times \text{PN}) / (R_0 \times T)$$

Where $\text{PE} = \%^{15}\text{N}$ enrichment of the PON fraction in excess of the natural abundance; $\text{PN} =$ particulate N concentration (mmol m^{-3}); $T =$ experimental duration (h) and R_0 is the calculated aqueous ^{15}N enrichment at time zero.

Phytoplankton distribution and nitrogen dynamics in the Southern Ocean

S. J. Thomalla et al.

Title Page

Abstract

Introduction

Conclusions

References

Tables

Figures

◀

▶

◀

▶

Back

Close

Full Screen / Esc

Printer-friendly Version

Interactive Discussion

3 Results

Northbound transect

3.1 Temperature distribution and frontal positions

On the northbound transect, the AF was positioned at approximately 40° S, while the STF was located at 43.5° S (Fig. 2a), further south than the range given by Lutjeharms and Valentine (1984). The AF and STF were present on this occasion as discrete fronts, separated by a warm core eddy (at 41.75° S) that had propagated downstream from the Agulhas retroflection zone. The presence and position of the eddy may account for the more southerly position of the STF on this transect. The SAF was located at 45.5° S. The bottom topography (Fig. 2b) illustrates the extent to which the ridge shallows in certain places (<1000 m).

3.2 Sea surface temperature and chlorophyll concentration

North of the AF, chl-*a* concentrations did not exceed $\sim 0.2 \text{ mg m}^{-3}$, while south of the AF, maximum concentrations of 0.4 mg m^{-3} were associated with the STF (Fig. 2c). There was no marked change in chl-*a* concentrations within the SAF region, although at $\sim 46^\circ \text{ S}$, in the shallow (<1000 m) region of the of the Prince Edward Island plateau, chl-*a* concentrations rose sharply to $\sim 1.6 \text{ mg m}^{-3}$. Nano- and pico-phytoplankton dominated (93%) phytoplankton biomass throughout the transect, except over the plateau where micro-phytoplankton dominated (81%) (Fig. 2d).

Southbound transect

3.3 General hydrography

Although the position of the AF was similar to that found on the northbound leg, it had now merged with the STF that had migrated equatorward during the intervening ten

days. The northward shift of the STF resulted from eastward movement of the warm eddy feature observed previously at 41.75° S.

Sloping isopycnals at about 38° S and 40° S (Fig. 3a) showed westwards and eastwards flow concentrated in relatively narrow bands. Westward flow at 38° S is thought to be part of a recirculation flow associated with a gap in the topography of the ridge (Pollard and Read, 2001). The concentrated eastward flow at 40° S separated subtropical surface water, lying along the TS line 15°C–35.5 to 24°C–34.6 (Darbyshire, 1966), from slightly fresher water found in the Agulhas Return Current and is considered to be the AF position (Read and Pollard, 1993; Park et al., 1993).

The depth of the surface mixed layer (SML) is defined by the steepest temperature gradient found at the base of the thermocline. North of the AF, warm surface waters (19.5–22°C) were isothermal to ~75 m, which marked the upper boundary of the strong seasonal thermocline. Below this, temperature dropped sharply to <17°C at 150 m (Fig. 3a). Water between 40.5–42.5° S is typical Agulhas water, however from 42.5° S to 43.25° S, there was a transitional region of fresh surface water (an Ekman layer driven north from the subantarctic zone) overlaying cooler central water (Fig. 3a,b). Temperatures at the base of the mixed layer (~12°C at ~80 m) are significantly less than those of Agulhas (15°C) or subtropical (19–20°C) water but higher than subantarctic waters (<9°C). The TS relation of this transitional region indicates mixing of Agulhas water and subantarctic surface water that probably mixed in the retroflexion zone.

On this transect the STF could be placed at the northern (42.5° S) or southern (43.25° S) edge of the transitional region. Both locations lie within a broad band of eastward flow (41°–46° S) indicated by upward sloping isopycnals, and neither is associated with any concentration of that flow. The more northerly edge marks the greatest change in water mass characteristics and concurs with the definitions outlined by Park et al. (1993) and hence the STF is placed at 42.5° S (Pakhomov et al., 1999). South of the STF, surface temperatures decrease to 8°C and the depth of the seasonal thermocline deepens to ~90 m at ~45.5° S.

Phytoplankton distribution and nitrogen dynamics in the Southern Ocean

S. J. Thomalla et al.

Title Page

Abstract

Introduction

Conclusions

References

Tables

Figures

⏪

⏩

◀

▶

Back

Close

Full Screen / Esc

Printer-friendly Version

Interactive Discussion



plateau ($\sim 0.74 \text{ mg m}^{-3}$). South of the STF, chl-*a* distribution showed considerable variation with a series of higher and lower concentrations. These changes in chl-*a* appear to be related to the potential temperature and salinity structure (Fig. 3a,b), with enhanced biomass coinciding with cold, fresh waters and vice versa. Such structures have been observed previously (Read and Pollard, 1993) and may possibly be attributed to eddies.

Surface chl-*a* concentrations (Fig. 4b) in subtropical waters north of the AF were low (max $\sim 0.23 \text{ mg m}^{-3}$) but increased over the AF and STF to ~ 0.27 and 0.38 mg m^{-3} , respectively, and to $\sim 0.74 \text{ mg m}^{-3}$ at the SAF. Elevated chl-*a* concentrations present at 46° S during the northbound transect were no longer evident at the same location 10 days later.

Integrated pigment concentrations to 150 m (Fig. 4c) show peaks in the concentration of all three size classes coinciding with the frontal regions. A summary of integrated and size fractionated chlorophyll data for the different regions is given in Table 2. South of the SAF, micro-phytoplankton are the dominant size class ($\sim 53\%$), while between the STF and SAF, pico- (57%) and nano-phytoplankton (31%) together account for $\sim 88\%$ of total pigment concentration, rising to $>97\%$ north of the AF. Apart from around the Prince Edward Island plateau, pico-phytoplankton are ubiquitous and the dominant fraction, extending their distribution to greater than 100 m depth.

3.5 Nutrient distribution

A strong gradient of increasing surface nitrate concentration is evident, with a progression from north to south across the region (Fig. 5a), concurrent with the decreasing temperature gradient (Fig. 3a). Nitrate values in subtropical surface waters are low ($< 1 \text{ mmol m}^{-3}$) and intensify southwards, with sharp increases in concentration across the STF ($2\text{--}4 \text{ mmol m}^{-3}$) and SAF ($8\text{--}11 \text{ mmol m}^{-3}$). By contrast, surface silicate (Fig. 5b) values remain low ($< 2 \text{ mmol m}^{-3}$) throughout the transect, with minimum concentrations ($< 1 \text{ mmol m}^{-3}$) at the STF and SAF. South of the SAF, surface

Phytoplankton distribution and nitrogen dynamics in the Southern Ocean

S. J. Thomalla et al.

Title Page

Abstract

Introduction

Conclusions

References

Tables

Figures

⏪

⏩

◀

▶

Back

Close

Full Screen / Esc

Printer-friendly Version

Interactive Discussion

(<~200 m) nitrate concentrations rise to 12–14 mmol m⁻³, but Si concentrations remain low (~2 mmol m⁻³), indicating uncoupling between uptake, regeneration and export processes. As expected, deeper waters below ~500 m are characterised by increasing nutrient concentrations that rise steadily down to 2000 m.

5 3.6 Phytoplankton new and regenerated production

Nutrient (NO₃⁻, NH₄⁺, urea) and N uptake data are presented for the nominal euphotic zone to the 0.1% light depth for six productivity stations (NP1–NP6) undertaken during the southbound transect. An exception is station NP1, which only has data up to the 1% light depth. The locations of these stations within hydrographic regions are given in Table.1. The ambient nutrient (NO₃, NH₄ and urea) concentrations, uptake rates, temperature and total chlorophyll are given in Table 3.

3.6.1 Ambient nitrate, ammonium and urea concentrations

Ambient nitrate, ammonium and urea concentrations were integrated over the euphotic zone and represented as a percentage of the total nitrogen pool (Fig. 6a–f). Changes in the nutrient regime occur with latitudinal progression and are most evident in the large NO₃ concentration differentials between subtropical and subantarctic waters. In subtropical waters (NP1–NP3) integrated NO₃ ranges from ~20 to 60 mmol m⁻² and comprises 20–30% of the total N pool. Further south, beyond the SAF, NO₃ concentrations continue to increase with latitude to a maximum of 1075 mmol m⁻² at the southern most station (NP6), where it constitutes 94% of total N.

Conversely, ambient urea decreased with southerly latitude, from a maximum in the north (NP1, 130.2 mmol m⁻²; 68% of total N), to a minimum in the south (NP6, 11.5 mmol m⁻²; just 1% of total N). Ambient NH₄⁺ concentrations were variable and displayed no obvious spatial trends. Station NP1 had the lowest ambient NH₄⁺

Phytoplankton distribution and nitrogen dynamics in the Southern Ocean

S. J. Thomalla et al.

Title Page

Abstract

Introduction

Conclusions

References

Tables

Figures

⏪

⏩

◀

▶

Back

Close

Full Screen / Esc

Printer-friendly Version

Interactive Discussion



(2.2 mmol m^{-2}), and comprised just over 1% of total N. The highest integrated values of 39.2 mmol m^{-2} and 59.9 mmol m^{-2} were found at the AF (NP3) and over the Prince Edward Island plateau (NP6).

3.6.2 Temperature and total chlorophyll profiles

5 Temperature and total chl-*a* profiles of the most northerly stations (NP1–NP3) show a stratified water column with a strong thermocline and shallow surface mixed layers (~60–75 m) that are shallower than the euphotic (0.1%) depth (Fig. 7a–c). To the south (NP4–NP6), the SML deepens to below the 0.1% light depth (>80 m), and the thermocline weakens, becoming almost isothermal at the most southerly station (NP6) (Fig. 7d–f). Stations NP1–NP3 have subsurface chl-*a* maxima that coincide with the
10 depth of the SML, while stations NP4–NP6 have surface chl-*a* maxima that decline rapidly below the 0.1% light depth.

3.6.3 Size fractionated chlorophyll distribution

15 Within subtropical waters of the ARC (NP1, NP2), total chl-*a* biomass was low (7.5 and 8.6 mg m^{-2}) and dominated by pico-phytoplankton (~80%). Micro-phytoplankton on the other hand only accounted for 2–4% of total chl-*a* (Fig. 8a,b). The AF (NP3) was marked by a sharp increase in biomass to 19.6 mg m^{-2} , but with little change in community structure (Fig. 8c). At the STF (NP4), biomass increased slightly with a shift towards nano-phytoplankton (~33%), the highest percentage recorded anywhere (Fig. 8d). Further south at stations NP5 and NP6, biomass rose to ~26 and
20 45 mg m^{-2} , respectively, and is attributable to larger micro-phytoplankton that dominated the community, accounting for 58.6% and 61.4% of total chl-*a* (Fig. 8e,f). The pico- (~22%) and nano-phytoplankton (~16%) size classes followed in relative abundance.

Phytoplankton distribution and nitrogen dynamics in the Southern Ocean

S. J. Thomalla et al.

Title Page

Abstract

Introduction

Conclusions

References

Tables

Figures

⏪

⏩

◀

▶

Back

Close

Full Screen / Esc

Printer-friendly Version

Interactive Discussion

3.6.4 Nitrogen uptake

Profiles of ρNO_3 , ρNH_4 and ρurea for the six productivity stations are shown in Fig. 9. ρN uptake rates were typically highest in surface (NP1, NP2, NP6) or subsurface (NP3, NP4, NP5) waters and decreased with depth to minimum values at the base of the euphotic layer. Integrated N uptake rates (Fig. 10a–f) illustrate the overall significance and percent contribution of each nutrient within the euphotic layer. Despite having the lowest mean total chl-*a* concentrations ($\sim 8 \text{ mg m}^{-2}$), the mean integrated total N uptake (ρN) rate at stations NP1 and NP2 was surprisingly high, attaining 29.9 and 23.7 $\text{mmol m}^{-2} \text{ d}^{-1}$, respectively (Fig. 10a,b). Urea and NH_4 dominated ρN , together contributing $\sim 94\%$ of ρN , while ρfNO_3 uptake ($\sim 6\%$) made only a minor contribution to the total. The AF (NP3) was marked by a tripling in water column ρN to 84.61 $\text{mmol m}^{-2} \text{ d}^{-1}$ but this was still dominated by regenerated ρN with ρfurea and ρfNH_4 contributing $\sim 46\%$ and $\sim 44\%$, respectively to ρN . The increased productivity is consistent with a doubling of the chl-*a* biomass to 19.6 mg m^{-2} relative to stations NP1 and NP2, although this does imply that chl-*a* specific uptake rates had become more efficient.

The STF station (NP4) did not fit the general trends. In spite of a similar total chl-*a* biomass (20.7 mg m^{-2}) to that at NP3 (AF), and an increase in ambient NO_3^- concentration (104.1 mmol m^{-2}), ρN was low (18.2 $\text{mmol m}^{-2} \text{ d}^{-1}$). Station NP5 within the SAF was also inconsistent, having the lowest ρN (7.1 $\text{mmol m}^{-2} \text{ d}^{-1}$) despite a high total chl-*a* biomass (25.8 mg m^{-2}) and a high ambient NO_3^- concentration (422.4 mmol m^{-2}).

Over the PE Island plateau (NP6), ρN was marked by an increase in ρN (to 55.2 $\text{mmol m}^{-2} \text{ d}^{-1}$), similar to rates within the AF (NP3). These high rates are consistent with the highest integrated chl-*a* value (45.3 mg m^{-2}), which was dominated by micro-phytoplankton ($\sim 61\%$) (Fig. 8f). Despite having a high micro-phytoplankton abundance, and the highest ρfNO_3 of all the stations ($\sim 14\%$), total ρN was still dominated by ρfNH_4 ($\sim 70.6\%$), while ρfurea was of the same order as ρfNO_3 and accounted for $\sim 15\%$ of ρN .

Phytoplankton distribution and nitrogen dynamics in the Southern Ocean

S. J. Thomalla et al.

Title Page

Abstract

Introduction

Conclusions

References

Tables

Figures

⏪

⏩

◀

▶

Back

Close

Full Screen / Esc

Printer-friendly Version

Interactive Discussion



3.6.5 *f*-ratios

f-ratio data for our study are illustrated in Fig. 11a–f. At subtropical stations NP1–NP3, the *f*-ratio generally increased with depth, tracking ambient NO₃ concentrations. Subsurface peaks in the *f*-ratio at 15 m coincided with increases in ambient NO₃ and with minimum concentrations of regenerated N. At the subtropical stations NP4 and NP5, the situation was reversed and *f*-ratios decreased with depth, indicating a shift from ρ NO₃ in surface waters to ρ N based primarily on reduced N at depth. However, the *f*-ratio profile for NP6, in relatively close proximity to the PE Islands and situated over the PE Island plateau, increased from a surface value of ~0.09 to a maximum of ~0.49 at the 0.1% light depth (96 m).

Integrated, but very low *f*-ratios (stations NP1–NP5 ranged from 0.04–0.11) (Fig. 12) indicate very strong regeneration based production, although there is a marginally increased reliance on ρ NO₃ in waters adjacent to the PE Islands (NP6), where the *f*-ratio increased to a maximum of 0.14.

4 Discussion

Our extensive latitudinal north-south transect to the south of Africa in late austral summer covered two hydrographically and biogeochemically distinct provinces; namely a subtropical region north of the STF and a subantarctic region south of the STF to as far south as the Prince Edward Island archipelago. Despite these distinctions, phytoplankton biomass was relatively uniform, but low, with only slight peaks in abundance observed at the frontal features and in the region of the Prince Edward Islands. Similarly, nitrogen uptake was also relatively low everywhere, with an overwhelming dominance by reduced nitrogen assimilation, as revealed by generally exceedingly low *f*-ratios. Almost everywhere too, nano- and pico-phytoplankton dominated community structure. In the following discussion, we deliberate regional differences and attempt to understand the biological, biogeochemical and hydrographic nuances that underpin our observations; with some speculative comment on the significance for POC export and CO₂ draw-down.

Phytoplankton distribution and nitrogen dynamics in the Southern Ocean

S. J. Thomalla et al.

Title Page

Abstract

Introduction

Conclusions

References

Tables

Figures

⏪

⏩

◀

▶

Back

Close

Full Screen / Esc

Printer-friendly Version

Interactive Discussion



4.1 Chlorophyll distribution and N assimilation north of the STF

Chlorophyll biomass in subtropical waters was low, with maximum concentrations $<0.3 \text{ mg m}^{-3}$. Throughout the region, pico-phytoplankton dominated chlorophyll size distribution ($>81\%$), followed by nano-phytoplankton ($\sim 16\%$) and an exceptionally low biomass of micro-phytoplankton ($\sim 3\%$) (Table 2).

Hydrographic characteristics for this region in late austral summer consisted of a shallow surface mixed layer ($\sim 75 \text{ m}$) of warm, salty subtropical water, separated from deeper water by a strong seasonal thermocline (Fig. 3a). Such vertical stratification prevents the transport of deeper NO_3 rich waters into the euphotic zone, except by shear or eddy diffusion, therefore accounting for low seasonal NO_3 ($<1 \text{ mmol m}^{-3}$) concentrations which are compounded by seasonal ρNO_3 that depletes the NO_3 pool (Fig. 5a). Silicate concentrations here were also low ($<1.5 \text{ mmol m}^{-3}$) and likely to limit diatom frustule formation (Fig. 5b).

Maximal NH_4 and urea concentrations (Fig. 6a–c) indicate that remineralisation rates exceeded nano- and pico-phytoplankton uptake rates for these nutrients (Dugdale and Goering, 1967; Tremblay et al., 2000). Primary production by micro-phytoplankton was limited by both NO_3 and silicate, thus paving the way for nano- and pico-phytoplankton dominated productivity based very strongly on regenerated N, as indicated by exceedingly low f -ratios (Figs. 11 and 12). This region also exhibited the highest chlorophyll- a normalised N uptake rates (ρN^*) (Fig. 13). For stations NP1 to NP3, north of the STF, the mean integrated ρN^* value was approximately 5 times that of the three subantarctic stations (NP4–NP6). These results could suggest that combined ρN and photosynthesis in the subantarctic is either Fe-limited or co-limited by Fe and light, where the latter encourages chl- a packaging to compensate for lowered light intensities, therefore resulting in lowered ρN^* values. Conversely, the region north of the STF appears to be freed from these influences.

f -ratio values north of the STF increased with depth alongside elevated ambient NO_3 concentrations (Fig. 11a–c) due to diffusive flux, indicating an increase in ρNO_3

OSD

7, 1347–1403, 2010

Phytoplankton distribution and nitrogen dynamics in the Southern Ocean

S. J. Thomalla et al.

Title Page

Abstract

Introduction

Conclusions

References

Tables

Figures

⏪

⏩

◀

▶

Back

Close

Full Screen / Esc

Printer-friendly Version

Interactive Discussion



**Phytoplankton
distribution and
nitrogen dynamics in
the Southern Ocean**S. J. Thomalla et al.

[Title Page](#)[Abstract](#)[Introduction](#)[Conclusions](#)[References](#)[Tables](#)[Figures](#)[⏪](#)[⏩](#)[◀](#)[▶](#)[Back](#)[Close](#)[Full Screen / Esc](#)[Printer-friendly Version](#)[Interactive Discussion](#)

with depth. This is unusual, although not unknown, since ρNO_3 is rather strongly light dependent and usually diminishes with depth (Lucas et al., 2007). It may be, therefore, that increasing ρNO_3 with depth, although potentially light limited, was offset by increasing NO_3 concentrations, and conceivably increased Fe concentrations that facilitated both photosynthesis and intracellular nitrate reduction, although this is purely speculative. Despite increasing nitrate utilisation near the thermocline however, no obvious increase in the micro-phytoplankton size fraction is observed and subsurface (~ 75 m) peaks in total chlorophyll continue to be dominated by small cells. As smaller pico- and nano-phytoplankton have a greater surface area to volume ratio than micro-phytoplankton, they are more efficient at scavenging potentially limiting nutrients, notably Fe, at low ambient concentrations (de Baar et al., 2005). Thus slow nutrient diffusion rates across the thermocline ensure that small cell sizes typically out-compete larger microphytoplankton, so accounting for their dominance at depth.

High concentrations of regenerated nutrients result from microzooplankton grazing control (Froneman and Perissinotto, 1996), and although small size confers a competitive advantage for nutrients at low concentrations, it also increases susceptibility to grazing by microzooplankton (Raven, 1986), which controls their biomass but nevertheless contributes to potential phytoplankton production based on ammonium excretion (Glibert et al., 1992). Thus the turnover rate of nano- and pico-phytoplankton is closely coupled to microzooplankton grazing and low nutrient concentrations, which control phytoplankton biomass accumulation in the subtropical region north of the STF, as previously noted by Froneman and Perissinotto (1996) and Bathmann et al. (2000) amongst others. One consequence of this ecosystem structure is that N is conserved, but respiratory CO_2 losses are high, and only a small fraction of the fixed POC is exported into deep water (Tremblay et al., 2000; Salter et al., 2007), not least because of the absence of any silicate ballasting effect (Thomalla et al., 2008; Sanders et al., 2010).

4.2 Chlorophyll distribution and N assimilation south of the STF

Crossing the STF into subantarctic surface water, total chlorophyll concentrations increase, but still remain low ($<0.7 \text{ mg m}^{-3}$), and although the community structure exhibits a higher proportion of micro-phytoplankton (Fig. 4c), nano- and pico-phytoplankton still remain the dominant components, except at the SAF and over the Prince Edward Island plateau.

The absence of a strong thermocline in subantarctic waters reduces vertical stability and allows deeper nutrient rich water to be mixed into the surface layer. South of 43° S the potential temperature and salinity sections (Fig. 3a,b) show considerable structure in a sequence from north to south, of cold, fresh and warm, salty features. These features are also apparent in the NO_3 and Si sections (Fig. 5a,b) and may result from anticyclonic shear-edge eddies of $\sim 200\text{--}300 \text{ km}$ in diameter. Their deep isothermal core results in substantial heat loss and convective overturning that entrains nutrients into surface waters (Dower and Lucas, 1993; Pollard et al., 2002), with the potential to enhance primary production wherever stability and stratification occurs.

Despite high NO_3 concentrations ($104\text{--}1074 \text{ mmol m}^{-2}$), primary production is still based primarily on regenerated nutrients as revealed by low f -ratios (<0.5) (Fig. 13), and dominated by pico- and nanophytoplankton cells ($\sim 68\%$). This scenario in Southern Ocean waters represents the now well-known high nutrient low chlorophyll (HNLC) paradox (Cullen, 1991) that is light-limited in winter and early spring, but Fe-limited in late spring and summer (Martin et al., 1989, 1991; de Baar et al., 1990, 2005; Moore et al., 2006, 2007a; Lucas et al., 2007; Cochlan, 2008).

4.2.1 Stratification and light limitation

The absence of a strong thermocline at this time meant that subantarctic waters were deeply mixed to $\sim 110 \text{ m}$ (Fig. 3a), substantially deeper than the average euphotic depth of $\sim 72 \text{ m}$. Irrespective of Fe availability, this leads to a situation where the mixing depth likely exceeded the critical depth and therefore limited phytoplankton growth (Nelson

OSD

7, 1347–1403, 2010

Phytoplankton distribution and nitrogen dynamics in the Southern Ocean

S. J. Thomalla et al.

Title Page

Abstract

Introduction

Conclusions

References

Tables

Figures

⏪

⏩

◀

▶

Back

Close

Full Screen / Esc

Printer-friendly Version

Interactive Discussion



and Smith, 1991). Apart from light-limited photosynthesis, nitrate uptake is also restricted by low irradiance (Morel, 1991; Probyn et al., 1996; Cochlan, 2008), as reflected here by the f -ratio profiles, which decrease with depth (Fig. 11d,e) because ρNO_3 is an energetically and therefore light sensitive process (see discussion in Lucas et al., 2007).

4.2.2 Preference and inhibition

It has been argued that when NH_4 is available to phytoplankton, ρNO_3 is suppressed (Glibert et al., 1982a,b; Dortch 1990), although relative NH_4 and Fe concentrations considerably complicate the issue (Lucas et al., 2007). Nonetheless, the interaction between ρNO_3 and ρNH_4 has hitherto been separated into an indirect preference for NH_4 and a direct inhibition of ρNO_3 (Dortch, 1990). Preference for NH_4 can be described by the relative preference index (RPI), which considers both the relative uptake rate and the relative concentration of a particular nutrient to provide an indication of the physiological preference by phytoplankton for that nutrient (McCarthy et al., 1977; Probyn, 1985). In this study, RPI results (Fig. 14) confirm the typical hierarchy of preference for $\text{NH}_4 > \text{urea} > \text{NO}_3$, reflecting the relative energetic costs of using oxidised versus reduced N sources. The relationship between regenerated N concentration and both ρNO_3 and the f -ratio (Fig. 15) suggests that high regenerated N concentrations ($\sim 3 \text{ mmol m}^{-3}$) inhibit ρNO_3 and therefore reduce the f -ratio. However, this conclusion is not unequivocal, since ρNO_3 could here be suppressed by Fe limitation, irrespective of NH_4 concentrations, as argued by Lucas et al. (2007).

4.2.3 Silicate limitation

Historically it has been argued that silicate (Si) may potentially limit diatom-based new production if present at concentrations $< 2 \text{ mmol m}^{-3}$ (Dugdale and Wilkerson, 1998). However, since Si concentrations can be driven to much less than this, it is more likely that ambient NO_3 :Si stoichiometry and the biogeochemical impacts of Fe-limited ρNO_3 determine residual Si concentrations (Moore et al., 2007b).

Phytoplankton distribution and nitrogen dynamics in the Southern Ocean

S. J. Thomalla et al.

Title Page

Abstract

Introduction

Conclusions

References

Tables

Figures

⏪

⏩

◀

▶

Back

Close

Full Screen / Esc

Printer-friendly Version

Interactive Discussion



In subantarctic surface waters of this region in late austral summer, Si limited productivity did appear to be significant, most likely because of the arguments outlined above (see also Smetacek, 1998). Nitrogen uptake rates only increased in the region of the Prince Edward Island plateau (station NP6) where Si concentrations were elevated and where Fe concentrations were most likely also elevated due to the same mechanisms seen downstream of the Crozet archipelago (Pollard et al., 2009). Such elevated concentrations of Si and Fe are likely responsible for the diatom-dominated micro-phytoplankton blooms found here (Figs. 16 and 8f).

4.2.4 Fe limitation

The control of phytoplankton productivity by iron availability in the HNLC Southern Ocean has been established through a series of in situ fertilisation experiments that show an increase in chlorophyll-*a* biomass and NO₃ “draw-down” after Fe additions. Such experiments include SOIREE (Boyd et al., 2000), EISENEX (Gervais et al., 2002), SOFEX (Caole et al., 2004) and EIFEX (Hoffmann et al., 2006). Naturally iron fertilised regions around the Crozet and Kerguelen Islands show very similar responses, including increased POC export in the Fe-enriched downstream regions (Blain et al., 2001, 2002, 2007; Pollard et al., 2009). Elevated chlorophyll concentrations downstream of these islands are also clearly visible from SeaWiFs ocean colour in early spring (Pollard et al., 2007), as it is around the Prince Edward Islands (Pollard et al., 2007). Although no iron measurements were made during this study, it is not unreasonable to suppose that the downstream regions of the Prince Edward Islands are also Fe-enriched, particularly during winter and in early spring (September, October). Around Crozet, the impact of Fe-enrichment on phytoplankton N metabolism waned significantly by early to mid summer (November to December) as surface Fe pools were depleted, resulting in a decline in the average *f*-ratio from ~0.45 to <0.2 (Lucas et al., 2007). A similar seasonal trend is also to be expected at the nearby and very similar latitude of the Prince Edward Islands. Given that this study was undertaken in April/May, in late

Phytoplankton distribution and nitrogen dynamics in the Southern Ocean

S. J. Thomalla et al.

Title Page

Abstract

Introduction

Conclusions

References

Tables

Figures



Back

Close

Full Screen / Esc

Printer-friendly Version

Interactive Discussion



summer, it is therefore not surprising that an expected iron mediated response in the f -ratio was barely observed.

4.3 Regions of enhanced biomass and productivity

The extent of the Southern Ocean makes it an area of great importance for the global ocean-atmosphere carbon balance despite its overall HNLC status. This is partly due to specific frontal, subantarctic island and ice-edge regions of the Southern Ocean that exhibit high seasonal rates of primary production; often by a diatom-dominated fraction (e.g., Bathmann et al., 2000; Tremblay et al., 2000; Atkinson et al., 2001; de Baar et al., 2005; Cochlan, 2008; Pollard et al., 2009). One result of this, for example, is that the APF, is associated with the greatest rate of biogenic silicate deposition in any of the world oceans. A further result is that the Southern Ocean exports (to 1000 m) the highest proportion (~3%) of its total production (Honjo et al., 2000), making it disproportionately important as a biologically mediated sink for atmospheric CO₂.

4.3.1 Enhanced biomass and productivity at ocean fronts

In this study, elevated surface chlorophyll concentrations coincided with frontal regions on both the northbound and southbound transects (Figs. 2c and 4b). Integrated chlorophyll during the southbound leg showed a significant peak just south of the STF, whereas peaks of lesser magnitude were associated with the SAF and the AF (Fig. 4c).

All three peaks in chlorophyll were strongly dominated by specific size classes, which suggest that the increase in biomass was probably the result of enhanced in situ production by selected components of the phytoplankton assemblage (Laubscher et al., 1993). The combination of strong horizontal temperature gradients, nutrient gradients, current velocities and sharp but shallow pycnocline boundaries tend to create the dynamical conditions most favourable for phytoplankton growth (Read et al., 2000).

Phytoplankton distribution and nitrogen dynamics in the Southern Ocean

S. J. Thomalla et al.

Title Page

Abstract

Introduction

Conclusions

References

Tables

Figures

⏪

⏩

◀

▶

Back

Close

Full Screen / Esc

Printer-friendly Version

Interactive Discussion

The Agulhas Front

The AF (NP3) was characterised by a doubling of chlorophyll biomass (Fig. 8c) and a 3-fold increase in water column N uptake (Fig. 10c) relative to adjacent non-frontal stations NP1 and NP2. However, ρ/N ($84.61 \text{ mmol m}^{-2} \text{ d}^{-1}$) was still dominated ($\sim 90\%$) by regenerated ρ/urea and ρ/NH_4 despite integrated NO_3 concentrations rising from ~ 19 (NP2) to $\sim 32 \text{ mmol m}^{-2}$ within the AF (NP3). Concurrently, the integrated f -ratio (Fig. 12) at NP3 was slightly higher (0.10) than at NP1 (0.06) and NP2 (0.04). Even so, little change was seen in phytoplankton community structure, which is consistent with subtropical waters dominated by pico-phytoplankton ($\sim 80\%$), fewer nano-phytoplankton and almost no micro-phytoplankton (Fig. 8c).

Despite the dominance of regenerated N uptake, the increased f -ratio within the AF implies a slight increase in ρNO_3 that could result from the observed increase in NO_3 flux, and/or from a more favorable light environment in the frontal region. Two potential mechanisms could introduce NO_3 into the surface mixed layer at the AF. As the Agulhas Current forms part of a shelf current, it exhibits meanders on various scales (Grundlingh, 1979; Lutjeharms et al., 1981). The first mechanism involves the presence of upwelling in the lee of such meanders, which may entrain nutrients into the euphotic zone. The second takes into consideration the kinematic nature of the Agulhas Current, whereby organisms living in the border-mixing area of a fast flowing current would experience a continuous but low rate of nutrient replenishment in areas of strong horizontal shear (Lutjeharms et al., 1985). These mechanisms of nutrient enrichment may account for the observed increase in integrated NO_3 concentration within the AF and for the biological enhancement found here (Fig. 6b,c).

The slow rate of NO_3 replenishment may limit micro-phytoplankton growth so that nano- and pico-phytoplankton dominated. However, pico-phytoplankton here exhibited the highest integrated ρN^* value ($4.32 \text{ mmol N (mg chl)}^{-1} \text{ m}^{-2} \text{ d}^{-2}$) of all productivity stations (Fig. 13), and are most likely outcompeting larger cells in scavenging the available NO_3 because of typically low K_s values associated with small cells (Eppley et al.,

OSD

7, 1347–1403, 2010

Phytoplankton distribution and nitrogen dynamics in the Southern Ocean

S. J. Thomalla et al.

Title Page

Abstract

Introduction

Conclusions

References

Tables

Figures

⏪

⏩

◀

▶

Back

Close

Full Screen / Esc

Printer-friendly Version

Interactive Discussion



1969). In the high light environment of the AF, increased per cell chlorophyll packaging is unnecessary, which will also tend to elevate ρN^* values. High irradiances also favour ρNO_3 , so both mechanisms may explain enhanced ρJN within the AF despite chlorophyll biomass being much higher at the STF and SAF.

5 The Subtropical Front

Previous studies of chlorophyll distribution across frontal boundaries have shown the STF to have consistently high biomass and rates of biological activity (e.g., Weeks and Shillington, 1994; Barange et al., 1998). Enhanced productivity has been recorded most often at the northern boundary between subtropical and subantarctic waters (Allanson and Parker, 1983; Lutjeharms et al., 1985; Laubscher et al., 1993), but this study shows a peak in chlorophyll concentration to the south of the STF at station NP4 (Fig. 4b,c). Pico- and nano-phytoplankton dominate, while micro-phytoplankton are largely absent (Fig. 8d). Nitrogen uptake within the community is based primarily on $\rho urea$ (56.5%) and ρNH_4 (37.6%) rather than on ρNO_3 (5.9%) (Fig. 10d).

The two most likely mechanisms responsible for biological enhancement at the STF depend on cross-frontal mixing. The first refers to mixing of nutrient-rich subantarctic surface water, from the well-mixed side of the frontal boundary, northwards across the STF to the more stratified side. Such increased nutrient supply into a more stratified and therefore more stable light environment promotes primary production and explains an observed increase in chlorophyll north of the STF (Plancke, 1977; Allanson et al., 1981; Lutjeharms, 1985). The second mechanism mixes warm, but nutrient poor water southwards across the STF, positively influencing the mixed layer depth and the light environment, but not necessarily the nutrient environment, unless there is a mechanism to entrain nutrients from below. The enhancement in vertical stability is expected to cause retention of phytoplankton in a high light environment and subsequent biomass accumulation associated with or just south of the STF.

If elevated pigment concentrations associated with ocean fronts are the result of favourable dynamical conditions, then enhanced rates of primary production would

Phytoplankton distribution and nitrogen dynamics in the Southern Ocean

S. J. Thomalla et al.

Title Page

Abstract

Introduction

Conclusions

References

Tables

Figures

⏪

⏩

◀

▶

Back

Close

Full Screen / Esc

Printer-friendly Version

Interactive Discussion



indicate a thriving population. This was however not the case at 43° S (NP4) within the chlorophyll bloom south of the STF, where productivity results show very low nutrient assimilation rates (Fig. 10d) and ρN^* rates (Fig. 13). These rates reflect a phytoplankton population that is both nutrient and light limited with a mixed layer depth that is well below the 0.1% light depth (Fig. 7d). Diatom growth at station NP4 would also be limited by very low integrated silicate values (2.3 mmol m^{-2}).

An alternative explanation of the chlorophyll peak situated one degree south of the STF is that it represents a senescent phytoplankton population, the zone of peak production associated with the front having migrated one degree further north. On the northbound transect 10 days previously; the STF was located at 43.5° S (Fig. 2a) and coincided with a two-fold increase in the surface total chlorophyll (Fig. 2c), and an increase in vertical stability with shallow surface mixed layer ($\sim 30 \text{ m}$). However, with the migration of the STF by one degree further north (42.5° S) on the southbound transect (Fig. 3a), the favourable conditions associated with the front, that are responsible for initialising and essential in maintaining enhanced productivity and biomass are no longer present at this location (43.5° S).

The Subantarctic Front

A peak in chlorophyll concentration (25.8 mg m^{-2}) coincides with the position of the SAF at 45° S (Fig. 4a–c). Total biomass is only slightly higher than at the AF and STF, however the community structure is significantly different (Fig. 8e) in that it is the first population to be dominated by the micro-phytoplankton size class ($>58\%$).

Laubscher et al. (1993) concluded that micro-phytoplankton blooms associated with the SAF probably occur as a result of cross frontal mixing of silicate into the surface layer. In our study, the prominence of micro-phytoplankton at the SAF coincided with depleted silicate concentrations in the euphotic surface layer to 12.2 mmol m^{-2} (Fig. 16). Combined with deep mixing and a low light environment (SML $>90 \text{ m}$, 0.1% $\sim 50 \text{ m}$), it is not surprising that ρfN values (7.1 mmol m^{-2}) were low for this SAF station (Fig. 10e).

Phytoplankton distribution and nitrogen dynamics in the Southern Ocean

S. J. Thomalla et al.

Title Page

Abstract

Introduction

Conclusions

References

Tables

Figures

⏪

⏩

◀

▶

Back

Close

Full Screen / Esc

Printer-friendly Version

Interactive Discussion



4.4 Enhanced biomass and N uptake in the vicinity of the Prince Edward Islands

Total chlorophyll concentrations (45.3 mg m^{-2}) at station (NP6) over the Prince Edward Island (PEI) shelf were the highest of all the productivity stations. Micro-phytoplankton dominated the community (61.4%) to attain the highest integrated biomass recorded (45.3 mg m^{-2}) for this size fraction, followed by pico- and nano-phytoplankton in relative abundance (Fig. 8f). Total ρ/N for this station (NP6) was high (Fig. 10f), second only to the AF (NP3) and dominated by ρNH_4 ($\sim 70.7\%$).

The f -ratio profile for this station (Fig. 11f) is somewhat anomalous since it increases from ~ 0.09 in surface waters to a maximum of ~ 0.49 at the 0.1% light depth (96 m). This can potentially be explained by the close proximity of this station to the Prince Edward Islands. Due to the high annual rainfall (up to 3000 mm), guano is dissolved primarily as urea, which is carried out to sea via run-off, along with NH_4 from the decomposition of detrital PON, thus elevating reduced nitrogen concentrations in near shore areas (Smith, 1987; Ismail, 1990). In support of these observations, this station was characterised by the highest concentration of NH_4 ($\sim 60 \text{ mmol m}^{-2}$) measured at any of the productivity stations (Fig. 6). Such high NH_4 concentrations (where ρNH_4 must be less than $r\text{NH}_4$) could potentially inhibit or suppress ρNO_3 in surface waters, particularly under conditions of low light and reduced N sufficiency (Dortch, 1990). Ambient NH_4 concentrations did not however show a significant decrease with depth (Table 3), which suggests that an additional mechanism is responsible for depth related changes in the f -ratio. Alternatively, or perhaps concurrently, the upward flux of dissolved Fe from shallow shelf sediments could encourage ρNO_3 at depth, provided that light is not limiting. Station NP6 is situated $\sim 16 \text{ km}$ north of Prince Edward Island, which despite being in relatively deep shelf waters ($\sim 1700 \text{ m}$) is situated downstream of the meandering SAF, which is steered past and north of the Islands by bottom topography (Ansorge et al., 1998). As such, it is likely that Fe is injected into the region from island run-off. A similar scenario is observed at the Crozet Islands, where

OSD

7, 1347–1403, 2010

Phytoplankton distribution and nitrogen dynamics in the Southern Ocean

S. J. Thomalla et al.

Title Page

Abstract

Introduction

Conclusions

References

Tables

Figures

⏪

⏩

◀

▶

Back

Close

Full Screen / Esc

Printer-friendly Version

Interactive Discussion

downstream increases in Fe from both benthic sediments and from island run-off result in elevated ρNO_3 and f -ratios north of the islands (Lucas et al., 2007; Pollard et al., 2009).

Micro-phytoplankton dominated communities observed at NP6 are likely to be alleviated from Fe stress, particularly in spring, and significant in terms of POC export, as is the case in the Fe-fertilised region of the Crozet Islands (Pollard et al., 2009; Bakker et al., 2007). This is borne out by elevated f -ratios. Furthermore, regionally elevated new production rates no doubt support the avifaunal and benthic community food webs, as well as creating a significant local and seasonal CO_2 “sink”.

5 Conclusions

Our north-south transect from subtropical to subantarctic waters revealed two regions of contrasting characteristics. The most conspicuous changes in chemical, physical and biological variables occurred at the STF, which separated the two regions. To the north, a warm, salty, highly stratified water column with low nitrate concentrations distinguished an eastern region of the subtropical South Atlantic, while the region south of the STF was characterised by cold nutrient-rich subantarctic surface waters of the Southern Ocean.

Subtropical waters were characterised by low concentrations of small phytoplankton cells and very low f -ratios, indicating productivity based almost entirely on recycled ammonium and urea. Diatom growth was probably limited by the strong seasonal thermocline, which creates sufficient vertical stratification to prevent the upward flux of nutrients into the euphotic zone. The biomass of small cells was most likely controlled by micro-zooplankton grazing, which was responsible for conserving reduced N pools, while respiratory CO_2 losses are high and POC export low. Biological CO_2 draw down is therefore minimal.

Crossing the STF into subantarctic surface waters, total chlorophyll concentrations increased and micro-phytoplankton became more prominent, although nano- and pico-phytoplankton still typically dominated. South of the STF, nutrient flux into surface

Phytoplankton distribution and nitrogen dynamics in the Southern Ocean

S. J. Thomalla et al.

Title Page

Abstract

Introduction

Conclusions

References

Tables

Figures



Back

Close

Full Screen / Esc

Printer-friendly Version

Interactive Discussion



Phytoplankton distribution and nitrogen dynamics in the Southern Ocean

S. J. Thomalla et al.

Title Page

Abstract

Introduction

Conclusions

References

Tables

Figures

◀

▶

◀

▶

Back

Close

Full Screen / Esc

Printer-friendly Version

Interactive Discussion



- Barange, M., Pakhomov, E. A., Perissinotto, R., Froneman, P. W., Verheye, H. M., Taunton-Clark, J., and Lucas, M. I.: Pelagic community structure of the subtropical convergence region south of Africa and in the mid-Atlantic Ocean, *Deep-Sea Res.*, 45, 1663–1687, 1998.
- Barrie, A., Davies, J. E., Park, A. J., and Workman, C. T.: Continuous-flows stable isotope analysis for biologists, *Spectroscopy*, 4, 42–52, 1989.
- Bathmann, U., Priddle, J., Treguer, P., Lucas, M. I., Parslow, J., and Hall, J.: Plankton ecology and biogeochemistry in the Southern Ocean: a first review of Southern Ocean JGOFS. in: *The Changing Ocean Carbon Cycle: a Midterm Synthesis of the Joint Global Ocean Flux Study*, edited by: Hanson, R. B., Ducklow, H. W., and Field, J. G., IGBP Book Series 5, Cambridge University Press, London, 2000.
- Belkin, I. M. and Gordon, A. L.: Southern Ocean fronts from the Greenwich meridian to Tasmania, *J. Geophys. Res.*, 101, 3675–3696, 1996.
- Blain, S., Treguer, P., Belviso, S., Bucciarelli, E., Denis, M., Desabre, S., Fial, M., Jézéquel, V. M., Le Fèvre, J., Mayzaud, P., Marty, J., and Razouls, S.: A biogeochemical study of the island mass effect in the context of the iron hypothesis: Kerguelen Islands, Southern Ocean, *Deep-Sea Res. Pt. II*, 48(1), 163–187, 2001.
- Blain, S., Queguiner, B., Armand, L., Belviso, S., Bombled, B., Bopp, L., Bowie, A., Brunet, C., Brussaard, C., Carlotti, F., Christaki, U., Corbiere, A., Durand, I., Ebersbach, F., Fuda, J., Garcia, N., Gerringa, L., Griffiths, B., Guigue, C., Guillerm, C., Jacquet, S., Jeandel, C., Laan, P., Lefevre, D., Lo Monaco, C., Malits, A., Mosseri, J., Obernosterer, I., Park, Y., Picheral, M., Pondaven, P., Remenyi, T., Sandroni, V., Sarthou, G., Savoye, N., Scouarnec, L., Souhaut, M., Thuiller, D., Timmermans, K., Trull, T., Uitz, J., van Beek, P., Veldhuis, M., Vincent, D., Viollier, E., Vong, L., and Wagener, T.: Effect of natural iron fertilization on carbon sequestration in the Southern Ocean, *Nature*, 446, 1070–1074, 2007.
- Boyd, P., Watson, A., Law, C., Abraham, E., Trull, T., Murdoch, R., Bakker, D., Bowie, A., Buesseler, K. O., Chang, H., Charette, M., Croot, P., Downing, K., Frew, R., Gall, M., Hadfield, M., Hall, J., Harvey, M., Jameson, G., LaRoche, J., Liddicoat, M., Ling, R., Maldonado, M., McKay, R. M., Nodder, S., Pickmere, S., Pridmore, R., Rintoul, S., Safi, K., Sutton, P., Strzepek, R., Tanneberger, K., Turner, S., Waite, A., and Zeldis, J.: A mesoscale phytoplankton bloom in the polar Southern Ocean stimulated by iron fertilization, *Nature*, 407, 695–702, 2000.
- Boyd, P. W., Jickell, T., Law, C. S., Blain, S., Boyle, E. A., Buesseler, K. O., Coale, K. H., Cullen, J. J., de Baar, H. J. W., Follows, M., Harvey, M., Lancelot, C., Levasseur, M.,

**Phytoplankton
distribution and
nitrogen dynamics in
the Southern Ocean**

S. J. Thomalla et al.

[Title Page](#)[Abstract](#)[Introduction](#)[Conclusions](#)[References](#)[Tables](#)[Figures](#)[◀](#)[▶](#)[◀](#)[▶](#)[Back](#)[Close](#)[Full Screen / Esc](#)[Printer-friendly Version](#)[Interactive Discussion](#)

Owens, N. P. J., Pollard, R., Rivkin, R. B., Sarmiento, J., Schoemann, V., Smetacek, V., Takeda, S., Tsuda, A., Turner, S., and Watson, A. J.: Mesoscale Iron enrichment experiments 1993–2005, *Synthesis and future directions*, *Science*, 315, 612–617, 2007.

Bury, S. J., Owens, N. J. P., and Preston, T.: ^{13}C and ^{15}N uptake by phytoplankton in the marginal ice zone of the Bellingshausen Sea, *Deep-Sea Res. Pt. II*, 42, 1225–1252, 1995.

Cochran, J. K., Buesseler, K. O., Bacon, M. P., Wang, H. W., Hirschberg, D. J., Ball, L., Andrews, J., Crossin, G., and Fleer, A. P.: Short-lived thorium isotopes (^{234}Th , ^{228}Th) as indicators of POC export and particle cycling in the Ross Sea, Southern Ocean, *Deep-Sea Res. Pt. II*, 47, 3451–3490, 2000.

Cochlan, W. P.: Nitrogen uptake in the Southern Ocean, 2nd edn., in: *Nitrogen in the Marine Environment*, edited by: Capone, D. G., Bronk, D. A., Mulholland, M. R., and Carpenter, E. J., Academic Press, Elsevier, 569–596, 2008.

Cullen, J. J.: Hypotheses to explain high-nutrient conditions in the open sea, *Limnol. Oceanogr.*, 36, 1578–1599, 1991.

Darbyshire, M.: The surface waters near the coasts of Southern Africa, *Deep-Sea Res.*, 13, 57–81, 1966.

De Baar, H. J. W., Buma, A. G. J., Nolting, R. F., Cadee, G. C., Jacques, G., and Treguer, P. J.: On iron limitation in the Southern Ocean: experimental observations in the Weddel and Scotia Seas, *Mar. Ecol.-Prog. Ser.*, 65, 105–122, 1990.

De Baar, H. J. W., Boyd, P. W., Coale, K. H., Landry, M. R., Tsuda, A., Assmy, P., Bakker, D. C. E., Bozec, Y., Barber, R. T., Brzezinski, M. A., Buesseler, K. O., Boye, M., Croot, P. L., Gervais, F., Gorbunov, M. Y., Harrison, P. J., Hiscock, W. T., Laan, P., Lancelot, C., Law, C. S., Levasseur, M., Marchetti, A., Millero, F. J., Nishioka, J., Nojiri, Y., Van Oijen, T., Riebesell, U., Rijkenberg, M. J. A., Saito, H., Takeda, S., Timmermans, K. R., Veldhuis, M. J. W., Waite, A. M., Wong, C. S. M., Bugg, W., Efremenko, Y., Kamyshev, Y., Kozlov, A., Nakamura, Y., Karwowski, H. J., Markoff, D. M., Nakamura, K., Rohm, R. M., Tornow, W., Wendell, R., Chen, M. J., Wang, Y. F., Piquemal, F., and Wong, C. S. D. M.: Synthesis of iron fertilization experiments: from the Iron Age in the Age of Enlightenment, *J. Geophys. Res.*, 110, C09S16, doi:10.1029/2004JC002601, 2005.

Diaz, F. and Raimbault, P.: Nitrogen regeneration and dissolved organic nitrogen release during spring in a NW Mediterranean coastal zone (Gulf of Lions): implications for the estimation of new production, *Mar. Ecol.-Prog. Ser.*, 197, 51–65, 2000.

Donald, K. M., Joint, I., Rees, A. P., Woodward, E. M. S., and Savidge, G.: Uptake of car-

Phytoplankton distribution and nitrogen dynamics in the Southern Ocean

S. J. Thomalla et al.

Title Page

Abstract

Introduction

Conclusions

References

Tables

Figures

◀

▶

◀

▶

Back

Close

Full Screen / Esc

Printer-friendly Version

Interactive Discussion



bon, nitrogen and phosphorus by phytoplankton along the 20° W meridian in the NE Atlantic between 57.5° N and 37° N, *Deep-Sea Res. Pt. II*, 48, 873–897, 2001.

Dore, J. E. and Karl, D. M.: Nitrification in the euphotic zone as a source for nitrite, nitrate, and nitrous oxide at station ALOHA, *Limnol. Oceanogr.*, 41, 1619–1628, 1996.

5 Dortch, Q.: The interaction between ammonium and nitrate uptake in phytoplankton, *Mar. Ecol.-Prog. Ser.*, 61, 183–201, 1990.

Dower, K. M. and Lucas, M. I.: Photosynthesis-irradiance relationships and production associated with a warm-core ring shed from the subtropical retroflection south of Africa, *Mar. Ecol.-Prog. Ser.*, 95, 141–154, 1993.

10 Dugdale, R. C. and Goering, J. J.: Uptake of new and regenerated forms of nitrogen in primary productivity, *Limnol. Oceanogr.*, 12(2), 196–206, 1967.

Dugdale, R. C. and Wilkerson, F. P.: Silicate regulation of new production in the equatorial Pacific upwelling, *Nature*, 391, 270–273, 1998.

Eppley, R., Rogers, J., and McCarthy, J.: Half-saturation constants for uptake of nitrate and ammonium by marine phytoplankton, *Limnol. Oceanogr.*, 14, 912–920, 1969.

Eppley, R. W. and Peterson, B. J.: Particulate organic matter flux and planktonic new production in the deep ocean, *Nature*, 282, 677–680, 1979.

Eppley, R. W.: New production: history, methods and problems, in: *Productivity of the Ocean: Present and Past*, edited by: Berger, W. H., Smetacek, V. S., and Wefer, G., John Wiley and Sons, New York, 85–97, 1989.

20 Fernandez, C. and Raimbault, P.: Nitrogen regeneration in the Northeast Atlantic Ocean and its impact on seasonal new, regenerated and export production, *Mar. Ecol.-Prog. Ser.*, 337, 79–92, 2007.

Froneman, P. W. and Perissinotto, R.: Microzooplankton grazing and protozooplankton community structure in the South Atlantic and in the Atlantic sector of the Southern Ocean, *Deep-Sea Res. Pt. I*, 43, 703–721, 1996.

Geider, R. J. and La Roche, J.: Redfield revisited: variability of C:N:P in marine microalgae and its biochemical basis, *Eur. J. Phycol.*, 37, 1–17, 2002.

Gervais, F., Riebesell, U., and Gorbunov, M. Y.: Changes in primary productivity and chlorophyll-*a* in response to iron fertilization in the Southern Polar Frontal Zone, *Limnol. Oceanogr.*, 47, 1324–1335, 2002.

30 Glibert, P. M., Biggs, D. C., and McCarthy, J. J.: Utilization of ammonium and nitrate during austral summer in the Scotia Sea, *Deep-Sea Res.*, 29, 837–850, 1982a.

**Phytoplankton
distribution and
nitrogen dynamics in
the Southern Ocean**

S. J. Thomalla et al.

[Title Page](#)[Abstract](#)[Introduction](#)[Conclusions](#)[References](#)[Tables](#)[Figures](#)[⏪](#)[⏩](#)[◀](#)[▶](#)[Back](#)[Close](#)[Full Screen / Esc](#)[Printer-friendly Version](#)[Interactive Discussion](#)

Deep-Sea Res., 31, 1461–1475, 1984.

Lutjeharms, J. R. E.: Location of frontal systems between Africa and Antarctica; some preliminary results, Deep-Sea Res., 32, 1499–1509, 1985.

Lutjeharms, J. R. E., Walters, N. M., and Allanson, B. R.: Oceanic frontal systems and biological enhancement, in: Antarctic Nutrient Cycles and Food Webs, edited by: Siegfried, W. R., Condy, P. R., and Laws, R. M., Springer-Verlag, Berlin, 11–21, 1985.

Lutjeharms, J. R. E. and Ansoerge, I. J.: The Agulhas return current, J. Marine Syst., 30(1–2), 115–138, 2001.

Martin, J. H. and Fitzwater, S.: Iron deficiency limits phytoplankton growth in the north-east Pacific subarctic, Nature, 331, 341–343, 1988.

Martin, J. H., Gordan, R., Fitzwater, S., and Brokenkow, W.: VERTEX: phytoplankton/iron studies in the Gulf of Alaska, Deep-Sea Res., 36, 649–680, 1989.

Martin, J. H., Gordon, R. M., and Fitzwater, S. E.: The case for iron, Limnol. Oceanogr., 36, 1793–1802, 1991.

Metzl, N., Tilbrook, B., and Poison, A.: The annual $f\text{CO}_2$ cycle and the air-sea CO_2 flux in the Sub-Antarctic Ocean, Tellus B, 51, 849–861, 1999.

Moore, C. M., Mills, M. M., Milne, A., Langlois, R., Achterberg, E. P., Lochte, K., Geider, R. J., and La Roche, J.: Iron limits primary productivity during spring bloom development in the central North Atlantic, Global Change Biol., 12, 626–634, 2006.

Moore, M. C., Seeyave, S., Hickman, A. E., Allen, J. T., Lucas, M. I., Planquette, H., Pollard, R., and Poulton, A. J.: Iron-light interactions during the CROZet natural iron bloom and EXport experiment (CROZEX) I: phytoplankton growth and photophysiology, Deep-Sea Res. Pt. II, 54, 2045–2065, 2007a.

Moore, M. C., Hickman, A. E., Poulton, A. J., Seeyave, S., and Lucas, M. I.: Iron-light interactions during the CROZet natural iron bloom and Export experiment (CROZEX) II: taxonomic responses and elemental stoichiometry, Deep-Sea Res. Pt. II, 54, 2066–2084, 2007b.

Morel, A.: Light and marine photosynthesis: a spectral model with geochemical and climatological implications, Prog. Oceanogr., 26, 263–306, 1991.

Morris, P. J., Sanders, R., Turnewitsch, R., and Thomalla, S.: ^{234}Th -derived particulate organic carbon export from an island-induced phytoplankton bloom in the Southern Ocean, Deep-Sea Res. Pt. II, 54, 2208–2232, 2007.

Nelson, D. M. and Smith, W. O.: Sverdrup re-visited: critical depths, maximum chlorophyll levels, and the control of Southern Ocean productivity by the irradiance-mixing regime, Limnol.

Phytoplankton distribution and nitrogen dynamics in the Southern Ocean

S. J. Thomalla et al.

Title Page

Abstract

Introduction

Conclusions

References

Tables

Figures

◀

▶

◀

▶

Back

Close

Full Screen / Esc

Printer-friendly Version

Interactive Discussion

Oceanogr., 36, 1650–1661, 1991.

Olson, R. J.: Differential photoinhibition of marine nitrifying bacteria: a possible mechanism for the formation of the primary nitrite maximum, *J. Mar. Res.*, 39, 227–238, 1981.

Owens, N. J. P. and Rees, A. P.: Determination of nitrogen-15 at submicrogram levels of nitrogen using automated continuous-flow isotope ratio mass spectrometry, *Analyst*, 114, 1655–1657, 1989.

Pakhomov, E. A., Froneman, P. W., and Ansoerge, I. J.: Prince Edward Islands' offshore oceanographic study: report of research cruise April–May 1997, *S. Afr. J. Sci.*, 94, 153–156, 1998.

Pakhomov, E. A., Ansoerge, I. J., McQuaid, C. D., Kohrs, S., Waldron, H., Hunt, B., Gurney, L., Kaehler, S., Lawrie, S., Held, C., and Machu, E.: The forth cruise of the Marion Island Oceanographic Survey (MIOS-IV), April–May 1999, *S. Afr. J. Sci.*, 95, 1–3, 1999.

Park, Y. H., Gamberoru, L., and Charriaud, E.: Frontal structure, water masses and circulation in the Crozet Basin, *J. Geophys. Res.*, 98, 12361–12385, 1993.

Parsons, T. R., Maita, Y., and Lalli, C. M.: *A Manual of Chemical and Biological Methods for Seawater Analysis*, Pergamon Press, Oxford, 173 pp., 1984.

Plancke, J.: Phytoplankton biomass and productivity in the subtropical convergence area and the shelves of the western Indian subantarctic islands, in: *Adaptions within Antarctic Ecosystems*, edited by: Liano, G. A., Smithsonian Institution, Washington, DC, 51–73, 1977.

Planquette, H., Statham, P. J., Fones, G. R., Charette, M. A., Moore, M., Salter, I., Nédélec, H., Taylor, S. L., French, M., Baker, A. R., Mahowald, N., and Jickells, T. D.: Dissolved iron in the vicinity of the Crozet Islands, Southern Ocean, *Deep-Sea Res. Pt. II*, 54, 1999–2019, 2007.

Pollard, R. T. and Regier, L. A.: Vorticity and vertical circulation at an ocean front, *J. Phys. Oceanogr.*, 22, 609–625, 1992.

Pollard, R. T. and Read, J. F.: Circulation pathways and transports of the Southern Ocean in the vicinity of the Southwest Indian Ridge, *J. Geophys. Res.*, 106, 2881–2898, 2001.

Pollard, R. T., Lucas, M. I., and Read, J. F.: Physical controls on biogeochemical zonation in the Southern Ocean, *Deep-Sea Res. Pt. II*, 49(16), 3289–3305, 2002.

Pollard, R., Sanders, R., Lucas, M., and Statham, P.: The Crozet natural iron bloom and export experiment (CROZEX), *Deep-Sea Res. Pt. II*, 54, 1905–1914, 2007.

Pollard, R. T., Salter, I., Sanders, R. J., Lucas, M. I., Moore, C. M., Mills, R. A., Statham, P. J., Allen, J. T., Baker, A. R., Bakker, D. C. E., Charette, M. A., Fielding, S., Fones, G. R., French, M., Hickman, A. E., Holland, R. J., Hughes, J. A., Jickells, T. D., Lampitt, R. S., Morris, P. J., Nedelec, F. H., Nielsdottir, M., Planquette, H., Popova, E. E., Poulton, A. J.,

Phytoplankton distribution and nitrogen dynamics in the Southern Ocean

S. J. Thomalla et al.

Title Page

Abstract

Introduction

Conclusions

References

Tables

Figures

⏪

⏩

◀

▶

Back

Close

Full Screen / Esc

Printer-friendly Version

Interactive Discussion



- Sanders, R., Morris, P., Stinchcombe, M., Seeyave, S., Venables, H. J., Lucas, M. I., and Moore, C. M.: New production and the f -ratio around the Crozet Plateau in austral summer 2004–5 diagnosed from seasonal changes in inorganic nutrient levels, *Deep-Sea Res. Pt. II*, 54, 2191–2207, 2007.
- 5 Sanders, R., Morris, P. J., Poulton, A. J., Stinchcombe, M. C., Charalampopoulou, A., Lucas, M. I., and Thomalla, S. J.: Does a ballast effect occur in the surface ocean?, *Geophys. Res. Lett.*, 37, L08602, doi:10.1029/2010GL042574, 2010.
- Schlitzer, R.: Ocean Data View, available at: <http://www.awi-bremerhaven.de/GEO/ODV> (last access: 13 May 2010), 2002.
- 10 Seeyave, S., Lucas, M. I., Moore, C. M., and Poulton, A. J.: Phytoplankton productivity and community structure across the Crozet Plateau, *Deep-Sea Res. Pt. II*, 54, 2020–2044, 2007.
- Smetacek, V.: Diatoms and the Silicate factor, *Nature*, 391, 224–225, 1998.
- Smith, V. R.: The environment and biota of Marion Island, *S. Afr. J. Mar. Sci.*, 83, 211–220, 1987.
- 15 Thomalla, S. J., Poulton, A. J., Sanders, R., Turnewitsch, R., Holligan, P. M., and Lucas, M. I.: Variable export fluxes and efficiencies for calcite, opal and organic carbon in the Atlantic Ocean: a ballast effect in action?, *Global Biogeochem. Cy.*, 22, GB1010, doi:10.1029/2007GB002982, 2008.
- Timmermans, K. R., van der Wagt, B., and de Baar, H. J. W.: Growth rates, half-saturation constants, and silicate, nitrate, and phosphate depletion in relation to iron availability of four large, open-ocean diatoms from the Southern Ocean, *Limnol. Oceanogr.*, 49(6), 2141–2151, 2004.
- Tremblay, J. E., Klein, B., and Legendre, L.: Estimation of f -ratios in oceans based on phytoplankton size structure, *Limnol. Oceanogr.*, 42, 595–601, 1997.
- 25 Tremblay, J. E., Legendre, L., Klein, B., and Therriault, J. C.: Size-differential uptake of nitrogen and carbon in a marginal sea (Gulf of St. Lawrence, Canada): significance of diel periodicity and urea uptake, *Deep-Sea Res. Pt. II*, 47, 489–518, 2000.
- Varela, M. M., Bode, A., Fernández, E., González, N., Kitidis, V., Varela, M., and Woodward, E. M. S.: Nitrogen uptake and dissolved organic nitrogen release in planktonic communities characterised by phytoplankton size-structure in the Central Atlantic Ocean, *Deep-Sea Res. I*, 52(9), 1637–1661, 2005.
- 30 Volk, T. and Hoffert, M. I.: Ocean carbon pumps: analysis of relative strengths and efficiencies in ocean-driven atmospheric CO₂ changes, in: *The Carbon Cycle and Atmospheric*

**Phytoplankton
distribution and
nitrogen dynamics in
the Southern Ocean**S. J. Thomalla et al.

[Title Page](#)[Abstract](#)[Introduction](#)[Conclusions](#)[References](#)[Tables](#)[Figures](#)[⏪](#)[⏩](#)[◀](#)[▶](#)[Back](#)[Close](#)[Full Screen / Esc](#)[Printer-friendly Version](#)[Interactive Discussion](#)

CO₂, Natural Variations Archean to Present, edited by: Sundguist, E. T. and Broeker, W. S., American Geophysical Union, Washington DC, 627 pp., 1985.

Waldron, H. N.: Influences on the hydrology of the Cape Columbine/St. Helena Bay region, M.Sc. thesis, University of Cape Town, 138 pp., 1985.

5 Waldron, H. N., Attwood, C. G., Probyn, T. A., and Lucas, M. I.: Nitrogen dynamics in the Bellinghousen Sea during the austral spring of 1992, Deep-Sea Res. Pt. II, 42, 1253–1276, 1995.

Weeks, S. J. and Shillington, F. A.: Interannual scales of variation of chlorophyll concentrations from CZCS data in the Benguela Upwelling System and the Subtropical Convergence south of Africa, J. Geophys. Res., 99, 7385–7399, 1994.

10 Whitworth, T. and Nowlin, W. D.: Water masses and currents of the Southern Ocean at the Greenwich Meridian, J. Geophys. Res., 92, 6462–6476, 1987.

Yool, A., Martin, A. P., Fernandez, C., and Clark, R. J.: Not so new: the significance of nitrification for oceanic “new” production, Nature, 447, 999–1002, 2007.

Phytoplankton distribution and nitrogen dynamics in the Southern Ocean

S. J. Thomalla et al.

Table 1. Sampling dates and positions of the six, productivity stations along the southbound transect. Note that station NP6 is on the Prince Edward Island (PEI) plateau.

Station Number	Date	Latitude (°S)	Longitude (°E)	Region
NP1	17 Apr 99	31 00.04	43 58.43	N of AF
NP2	19 Apr 99	37 00.20	43 58.33	N of AF
NP3	20 Apr 99	40 00.43	44 02.27	AF
NP4	23 Apr 99	43 01.02	40 57.36	STF
NP5	24 Apr 99	45 20.60	38 44.18	SAF
NP6	24 Apr 99	46 30.28	37 52.37	PEI plateau

Title Page

Abstract

Introduction

Conclusions

References

Tables

Figures

⏪

⏩

◀

▶

Back

Close

Full Screen / Esc

Printer-friendly Version

Interactive Discussion



Table 2. Maximum chlorophyll concentrations and size fractionated phytoplankton distribution for the subtropical and subantarctic regions north and south of the STF, respectively. Size ranges are fractionated as follows: micro- (>20–200 μm), nano- (2–20 μm) and pico- (<2.0 μm) phytoplankton.

Chlorophyll within the top 150 m (mg m^{-3})				
Region	Max	Micro (%)	Nano (%)	Pico (%)
N of STF	0.27	2.8	16.0	81.3
S of STF	0.74	32.4	24.8	42.9

t2

Phytoplankton distribution and nitrogen dynamics in the Southern Ocean

S. J. Thomalla et al.

Title Page

Abstract Introduction

Conclusions References

Tables Figures

⏪ ⏩

◀ ▶

Back Close

Full Screen / Esc

Printer-friendly Version

Interactive Discussion



Phytoplankton distribution and nitrogen dynamics in the Southern Ocean

S. J. Thomalla et al.

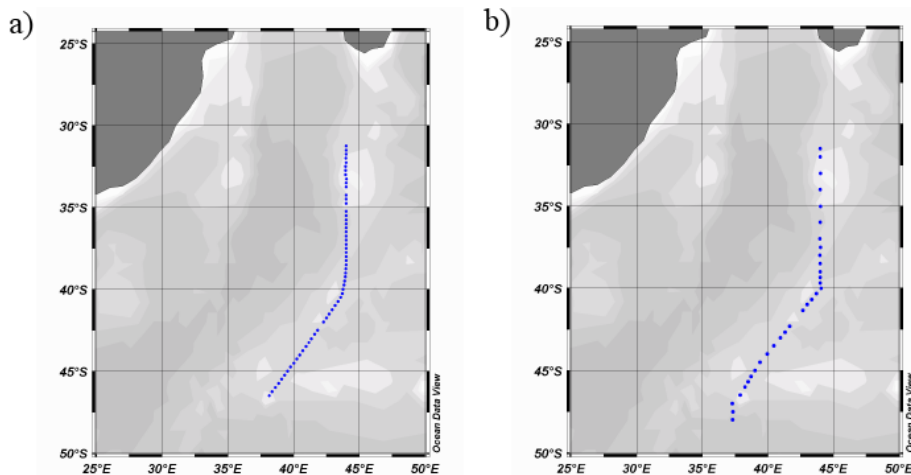


Fig. 1. (a) Cruise track and XBT station positions for the northbound transect from the Prince Edward Islands to 31° S and (b) cruise track and CTD station positions for the southbound transect.

[Title Page](#)[Abstract](#)[Introduction](#)[Conclusions](#)[References](#)[Tables](#)[Figures](#)[⏪](#)[⏩](#)[◀](#)[▶](#)[Back](#)[Close](#)[Full Screen / Esc](#)[Printer-friendly Version](#)[Interactive Discussion](#)

Phytoplankton distribution and nitrogen dynamics in the Southern Ocean

S. J. Thomalla et al.

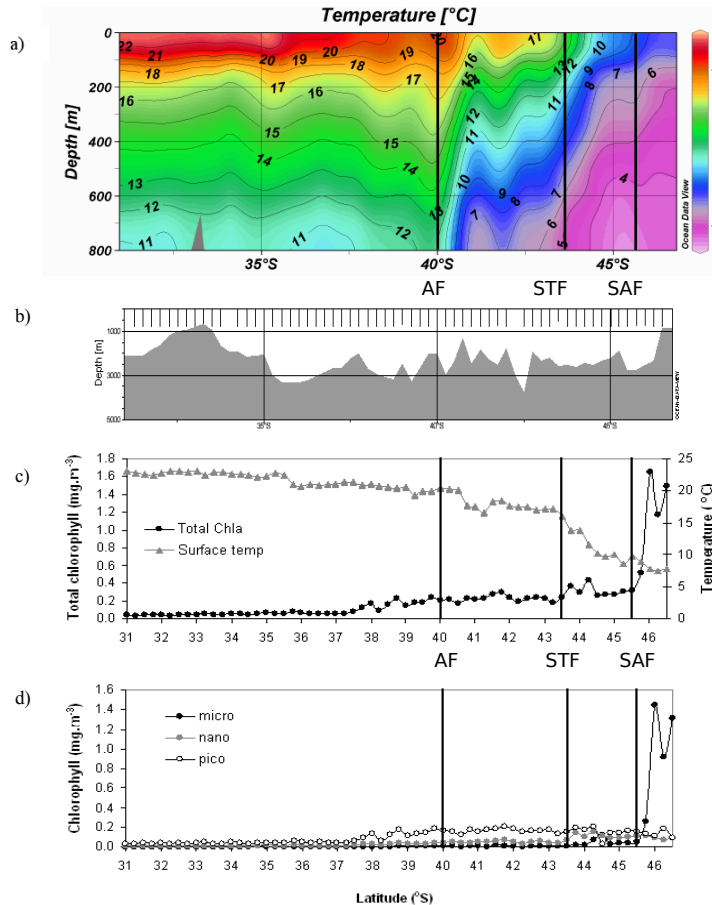


Fig. 2. (a) XBT temperature section during the northbound transect, (b) topography section shows the position and depth of each XBT station, (c) surface chlorophyll (mg m^{-3}) and sea surface temperature ($^{\circ}\text{C}$) distribution and (d) size fractionated distribution (mg m^{-3}) of the surface phytoplankton population along the northbound transect. The position of the Agulhas Front (AF), Subtropical Front (STF) and Subantarctic Front (SAF) are indicated as bold lines. Plots made using Ocean Data View (Schlitzer, 2004).

Phytoplankton distribution and nitrogen dynamics in the Southern Ocean

S. J. Thomalla et al.

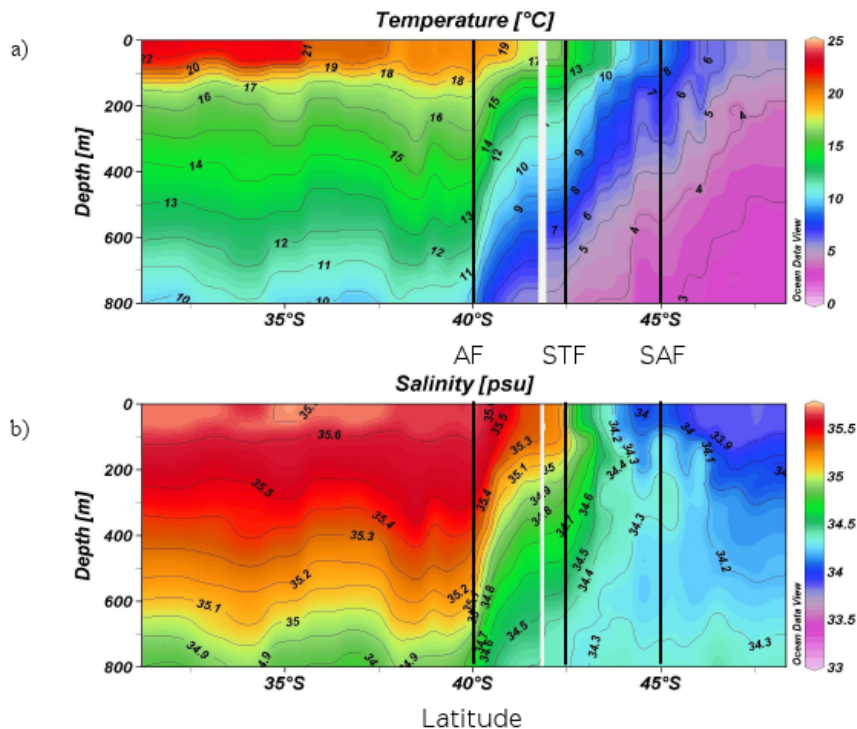


Fig. 3. Sections to 800 m of **(a)** temperature (°C) and **(b)** salinity (psu) for the southbound transect between 31° S and the Prince Edward Islands.

Title Page

Abstract

Introduction

Conclusions

References

Tables

Figures

◀

▶

◀

▶

Back

Close

Full Screen / Esc

Printer-friendly Version

Interactive Discussion

Phytoplankton
distribution and
nitrogen dynamics in
the Southern Ocean

S. J. Thomalla et al.

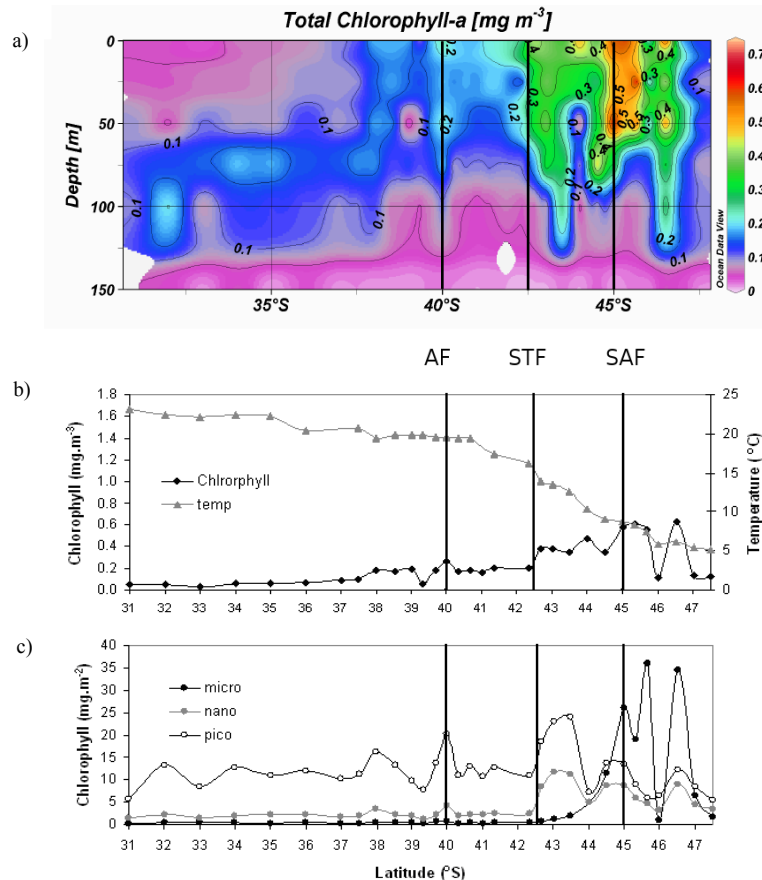


Fig. 4. (a) CTD total chlorophyll (mg m^{-3}) section to 150 m (b) sea surface temperature ($^{\circ}\text{C}$) and total surface chlorophyll distribution (mg m^{-3}) and (c) size fractionated chlorophyll distribution (mg m^{-3}) integrated over the top 150 m for the southbound transect. The position of the three frontal systems and the productivity stations NP1–NP6 are indicated.

Phytoplankton distribution and nitrogen dynamics in the Southern Ocean

S. J. Thomalla et al.

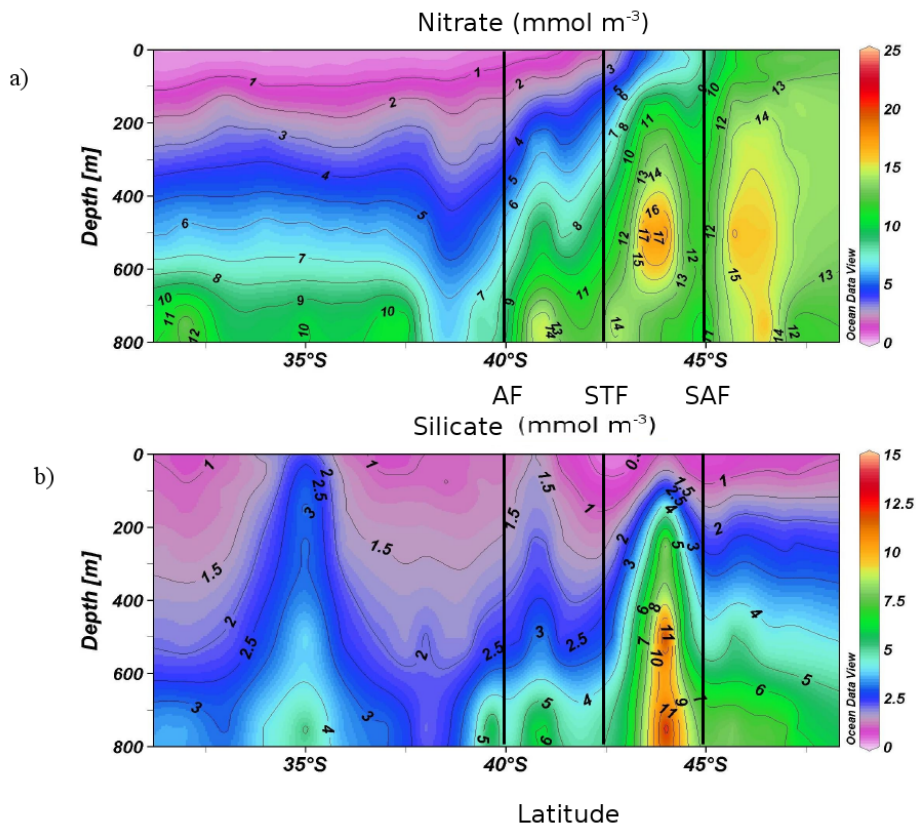


Fig. 5. (a) Nitrate (mmol m^{-3}) and (b) silicate (mmol m^{-3}) sections to 800 m for the southbound transect. The three fronts crossed during the transect are marked as bold lines.

Title Page

Abstract

Introduction

Conclusions

References

Tables

Figures

◀

▶

◀

▶

Back

Close

Full Screen / Esc

Printer-friendly Version

Interactive Discussion

Phytoplankton
distribution and
nitrogen dynamics in
the Southern Ocean

S. J. Thomalla et al.

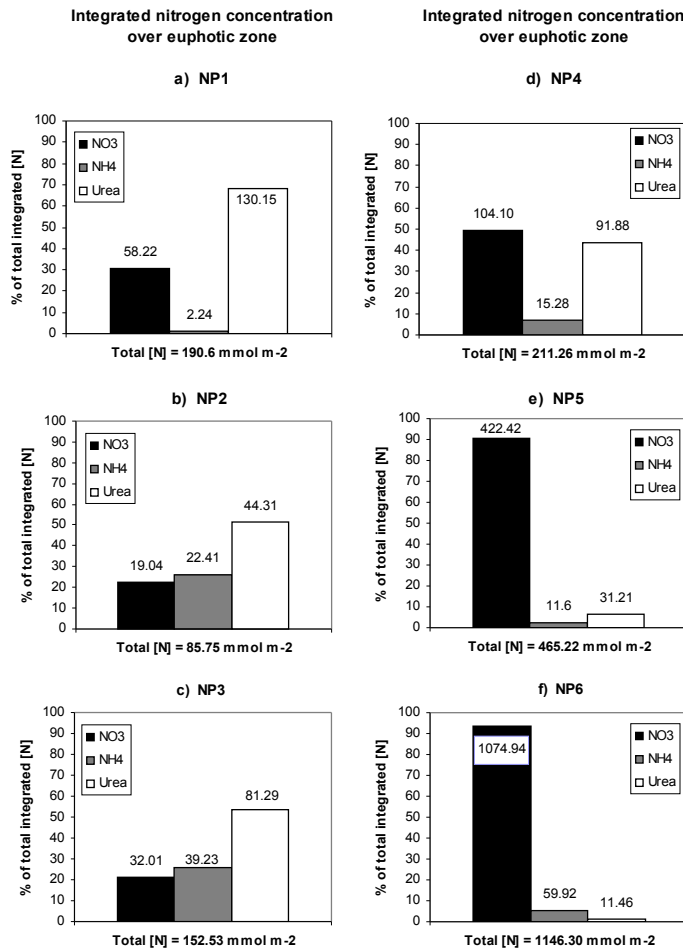


Fig. 6. Integrated (to the 0.1% light depth) measurements of nitrate, ammonium and urea (mmol m^{-2}) concentrations represented as a percentage of the total ambient nitrogen, for each of the six productivity stations.

Phytoplankton distribution and nitrogen dynamics in the Southern Ocean

S. J. Thomalla et al.

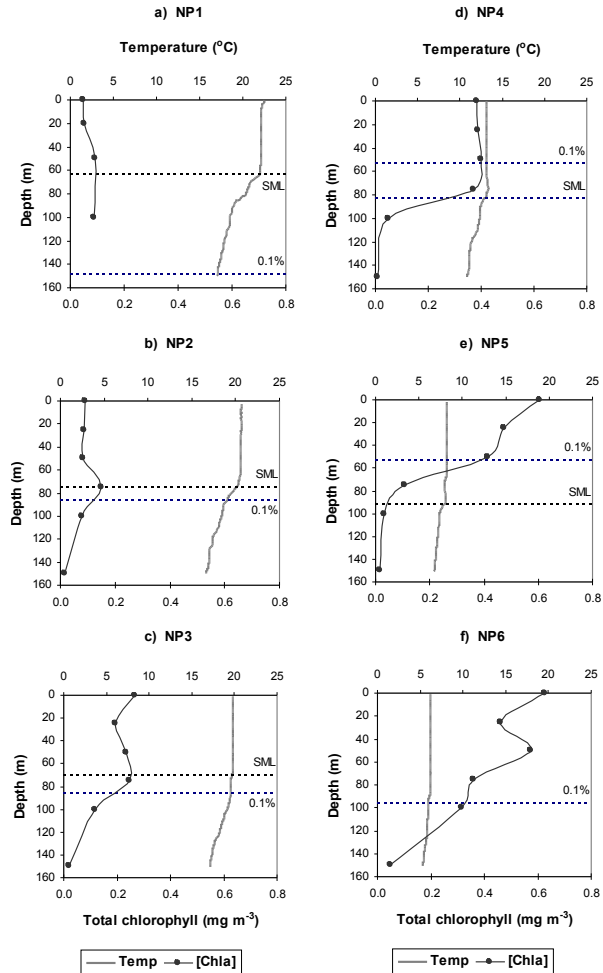


Fig. 7. Vertical profiles of temperature (°C) and total chlorophyll (mg m⁻³) for the top 150 m of each productivity station on the southbound transect. Together with surface mixed layer and euphotic (0.1% light) depths.

[Title Page](#)
[Abstract](#)
[Introduction](#)
[Conclusions](#)
[References](#)
[Tables](#)
[Figures](#)
[◀](#)
[▶](#)
[◀](#)
[▶](#)
[Back](#)
[Close](#)
[Full Screen / Esc](#)
[Printer-friendly Version](#)
[Interactive Discussion](#)

Phytoplankton distribution and nitrogen dynamics in the Southern Ocean

S. J. Thomalla et al.

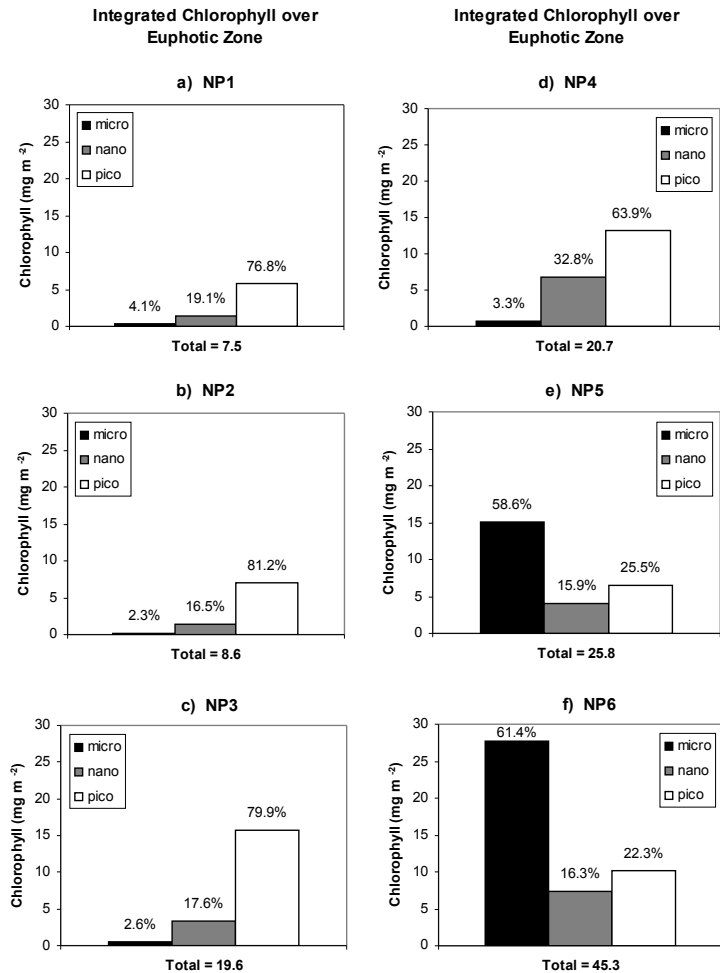


Fig. 8. Euphotic zone integrated measurements of size-fractionated chlorophyll concentration (mg m^{-2}) for the six productivity stations on the southbound transect.

Phytoplankton distribution and nitrogen dynamics in the Southern Ocean

S. J. Thomalla et al.

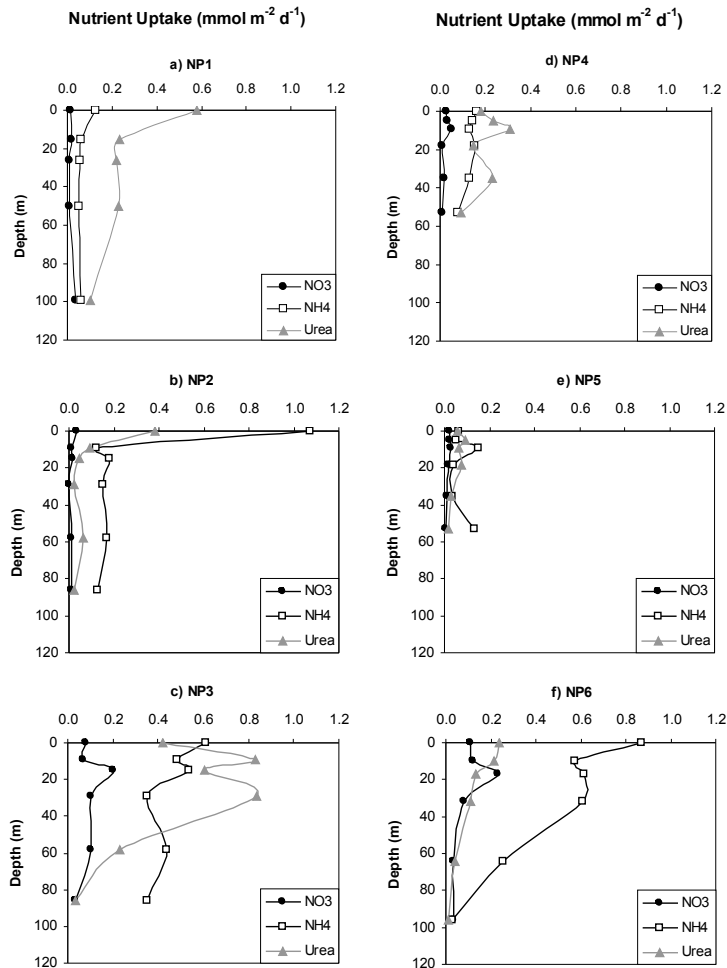


Fig. 9. Vertical profiles of nitrate, ammonium and urea uptake rates (mmol m⁻³) for the six productivity stations on the southbound transect.

[Title Page](#)
[Abstract](#)
[Introduction](#)
[Conclusions](#)
[References](#)
[Tables](#)
[Figures](#)
[◀](#)
[▶](#)
[◀](#)
[▶](#)
[Back](#)
[Close](#)
[Full Screen / Esc](#)
[Printer-friendly Version](#)
[Interactive Discussion](#)

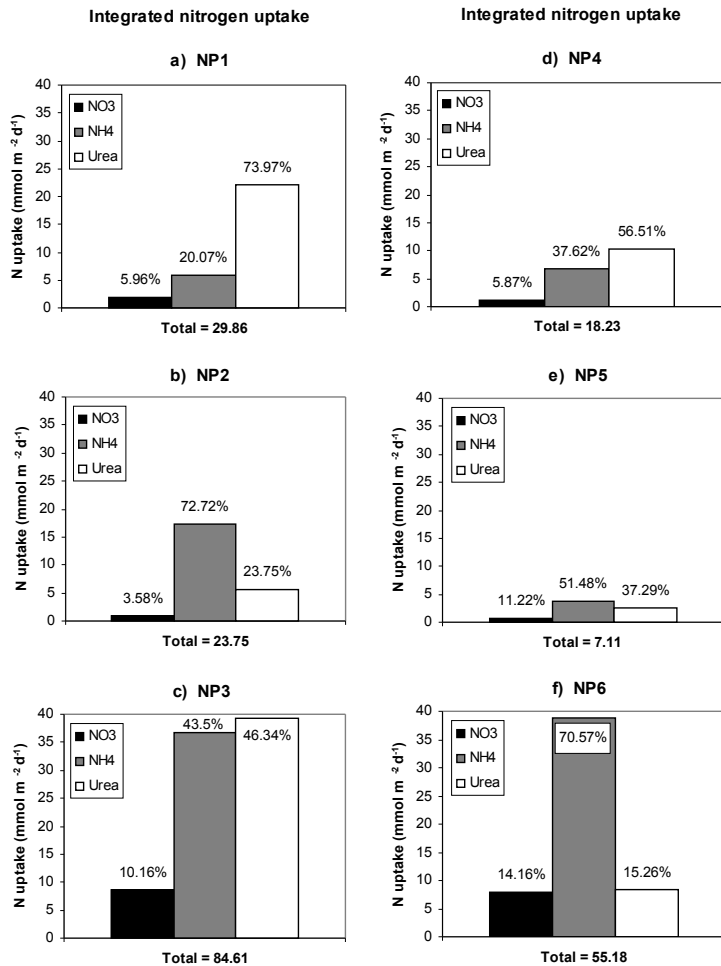


Fig. 10. Euphotic zone integrated measurements of nitrate, ammonium and urea uptake ($\text{mmol m}^{-2} \text{d}^{-1}$) for productivity stations NP1–NP6.

Phytoplankton
distribution and
nitrogen dynamics in
the Southern Ocean

S. J. Thomalla et al.

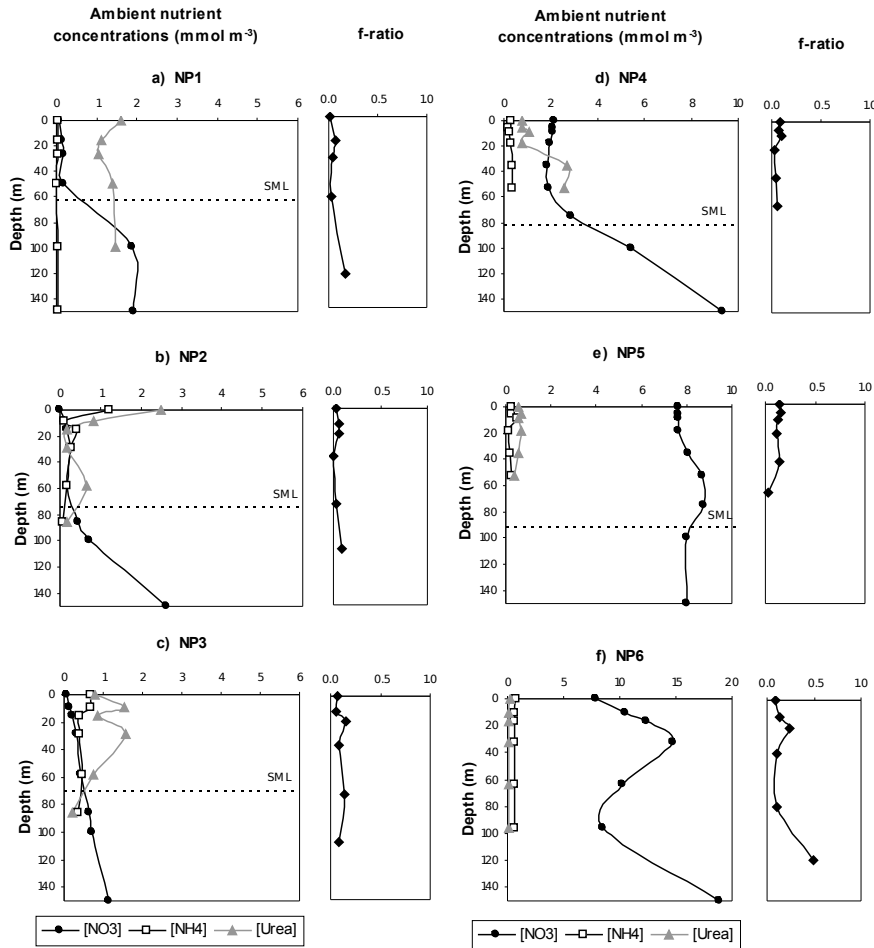


Fig. 11. Vertical profiles of nitrate, ammonium and urea concentrations (mg-at m^{-3}) for productivity stations NP1–NP6 together with vertical f -ratio profiles for each station. Notice the change in nutrient concentration axis scale for stations NP4, NP5 and NP6.

Phytoplankton distribution and nitrogen dynamics in the Southern Ocean

S. J. Thomalla et al.

Title Page

Abstract

Introduction

Conclusions

References

Tables

Figures

⏪

⏩

◀

▶

Back

Close

Full Screen / Esc

Printer-friendly Version

Interactive Discussion

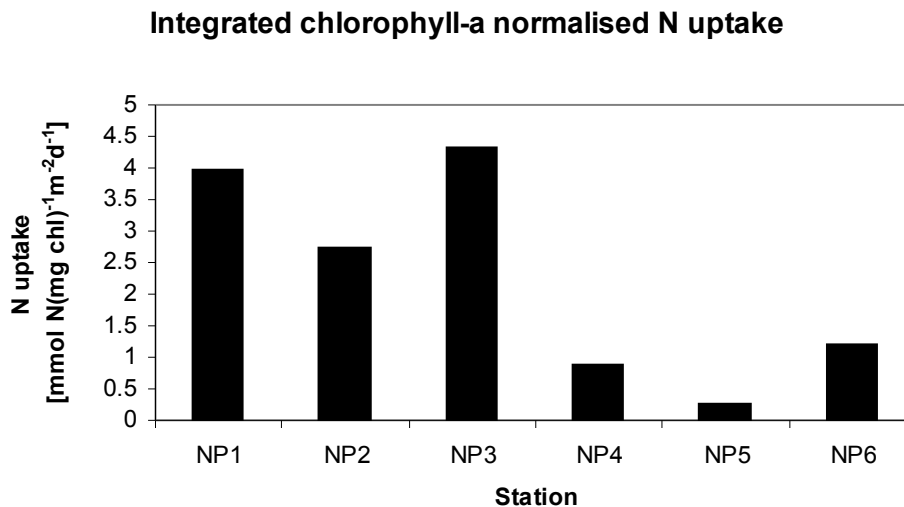


Fig. 13. Euphotic zone integrated chlorophyll-a normalized nitrogen uptake ($\text{mmol-at N (mg chl)}^{-1} \text{m}^{-2} \text{d}^{-1}$) for the six productivity stations of the southbound transect.

**Phytoplankton
distribution and
nitrogen dynamics in
the Southern Ocean**

S. J. Thomalla et al.

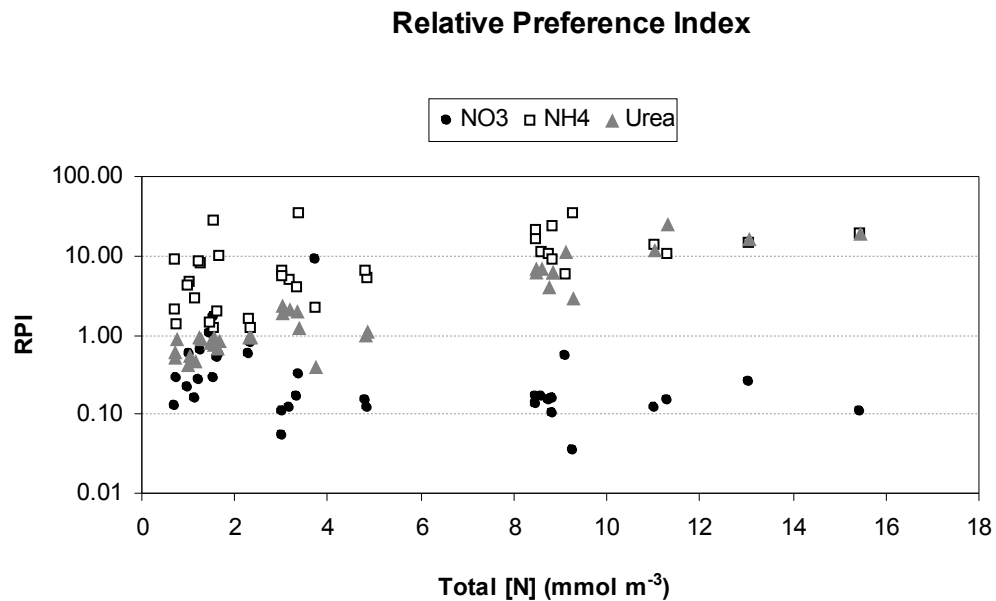


Fig. 14. Relative Preference Index (RPI) plotted against total nitrogen concentration (mmol m^{-3}) for the six productivity stations.

Title Page

Abstract

Introduction

Conclusions

References

Tables

Figures

◀

▶

◀

▶

Back

Close

Full Screen / Esc

Printer-friendly Version

Interactive Discussion

**Phytoplankton
distribution and
nitrogen dynamics in
the Southern Ocean**

S. J. Thomalla et al.

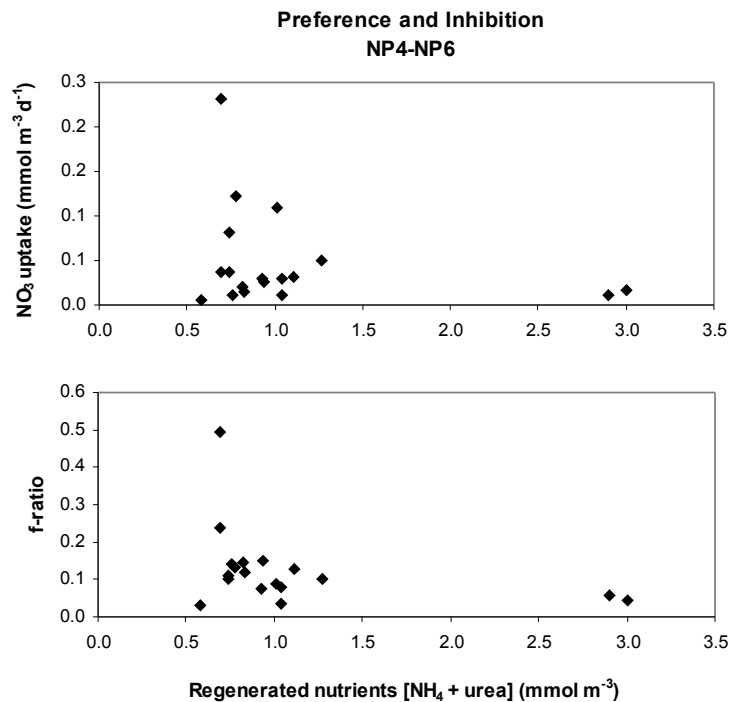


Fig. 15. Relationship between new production ($\text{mmol m}^{-3} \text{d}^{-1}$) and ambient regenerated nutrient concentration (mmol m^{-3}) for subantarctic stations NP4, NP5 and NP6.

Phytoplankton distribution and nitrogen dynamics in the Southern Ocean

S. J. Thomalla et al.

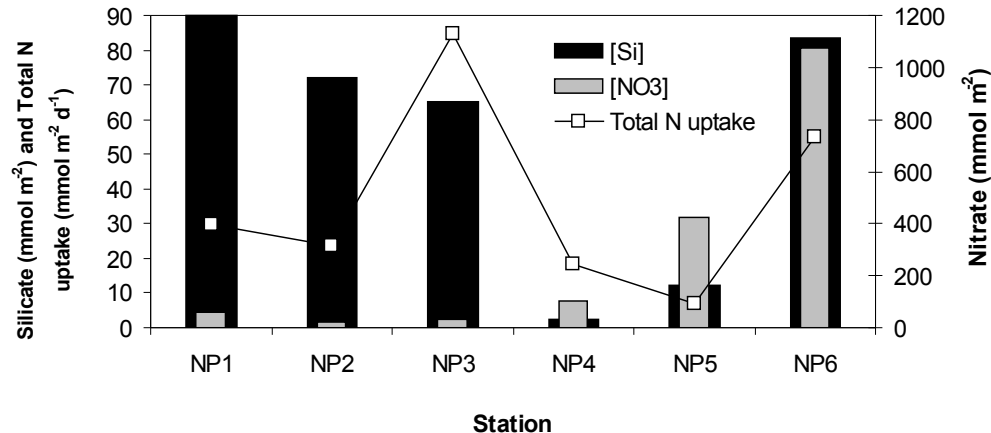


Fig. 16. Relationship between total nitrogen uptake ($\text{mmol m}^{-2} \text{d}^{-1}$) and integrated nitrate and silicate concentrations (mmol m^{-2}) for the euphotic zone, from station NP1 at 31°S to NP6 in the region of the Prince Edward Islands. Note that the integrated silicate concentration at station NP1 (563 mmol m^{-2}) exceeds the y axis of the figure.

Title Page

Abstract Introduction

Conclusions References

Tables Figures

◀ ▶

◀ ▶

Back Close

Full Screen / Esc

Printer-friendly Version

Interactive Discussion